Achieving highly efficient gene transfer to the bladder by increasing the molecular weight of polymer-based nanoparticles

Gang Li[a,b,‡], Shanshan He[a,1,‡], Andreas G. Schätzlein[b], Robert M. Weiss[a], Darryl T. Martin[a,*], and Ijeoma F. Uchegbu[b,*].

[a]Department of Urology, Yale University, New Haven, CT; and [b]School of Pharmacy, University College London, London, UK.

Present Address: [1]Department of Breast Reconstruction, Tianjin Medical University Cancer Institute and Hospital, National Clinical Research Center for Cancer, Key Laboratory of Cancer Prevention and Therapy, Tianjin, China.

[‡]These authors contributed equally to this work.

* These authors contributed equally to this work and are whom correspondence should be addressed.

Ijeoma F. Uchegbu | Tel: +44 207 753 5997; Fax: +44 207 753 5942; email: ijeoma.uchegbu@ucl.ac.uk

Darryl T. Martin | Tel +1 203.785.4195; Fax: +1 203.785.4043; email: darryl.martin@yale.edu

Short title: Higher molecular weight polymer enables bladder gene delivery

Abstract

Short dwell-time and poor penetration of the bladder permeability barrier (BPB) are the main obstacles to intravesical treatments for bladder diseases, and is evidenced by the lack of such therapeutic options on the market. Herein, we demonstrate that by finely tuning the molecular weight of our cationic polymer mucoadhesive nanoparticles, we enhanced our gene transfer, leading to improved adherence and penetrance through the BPB in a safe and efficient manner. Specifically, increasing the polymer molecular weight from 45 kDa to 83 kDa enhanced luciferase plasmid transfer to the healthy murine bladder, leading to 1.35 ng/g luciferase protein expression in the urothelium and lamina propria regions. The relatively higher molecular weight polymer (83 kDa) did not induce morphologic changes or inflammatory responses in the bladder. This approach of altering polymer molecular weight for prolonging gene transfer residence time and deeper penetration through the BPB could be the basis for the design of future gene therapies for bladder diseases.

Keywords

List of Abbreviations

β-gal-pDNA	Beta-galactosidase plasmid
Cy5	Cyanine5
DAB	3,3'-diaminobenzidine
DOPE	1,2-dioleoyl-sn-glycero-3-phosphoethanolamine
EAGC	N-(2-ethylamino)-6-O-glycolchitosan)
EGCDNPs	EAGC-DOPE lipid hybrid nanoparticles
FBS	Fetal bovine serum
FLuc-pDNA	Firefly luciferase plasmid
γ-H2AX	Gamma-H2AX
GC	Glycol chitosan
GFP-pDNA	Green fluorescent protein plasmid
GP130	Glycoprotein-130
H & E	Hematoxylin and eosin
IHC	Immunohistochemistry
Lipo 2k	Lipofectamine 2000
MPO	Myeloperoxidase
NMR	Nuclear magnetic resonance
PLGA	Poly(lactic-co-glycolic acid)
PVDF	Polyvinylidene fluoride
siRNA	Small interfering RNA
siGP130	GP130 siRNA
TEM	Transmission electron microscopy

1. Introduction

Over eighteen million new cases of cancer are diagnosed worldwide annually [1]. Amongst these, approximately 550,000 patients were diagnosed with bladder cancer and around 200,000 deaths were reported [1, 2]. In the US, bladder cancer deaths are expected to rise to approximately 18,000 in 2020 [3]. Seventy to 80% of bladder cancer patients have non-muscle invasive (NMIBC), and up to 25% of NMIBC patients will progress to muscle invasive bladder cancer (MIBC), despite aggressive treatment interventions such as maximum tumor resection [4]. Due to this high tendency to progress to MIBC, patients diagnosed with NMIBC are committed to lifelong surveillance consisting of urine cytology and cystoscopy, making it one of the most expensive cancers to manage with a projected total cost of $5 billion in the US by 2020 [5]. This course of events significantly impacts the patient's quality of life and imposes a heavy financial burden on society.

Patients with NMIBC are intravesically treated with attenuated vaccines, such as Bacillus Calmette-Guérin (BCG) derived from the *Mycobacterium bovis* [6]. However, up to 50% of patients do not respond to BCG, which increases the risk of disease progression [7]. Mitomycin C, doxorubicin, epirubicin, and gemcitabine also have been employed to intravesically treat NMIBC [8-10]. The short drug dwell-time due to voiding and poor penetration of the drug into the tumor and bladder wall, however, results in the need for repeated intravesical instillations of the chemotherapeutics [10]. The frequent repeated dosing of cisplatin in a prospective randomized study resulted in chemical cystitis and triggered an anaphylactic reaction [11]. To date, no platinum-based chemotherapy has been approved in the US to treat NMIBC intravesically. However, there are preclinical mouse model studies being performed testing nanoparticle delivery platforms encapsulating cisplatin for intravesical delivery [12, 13].

In order to improve drug delivery to the tumor and reduce the severe side effects of frequent dosing, intravesical gene therapy (or gene transfer) has been advocated as a promising

alternative approach to the treatment of bladder cancer. Improved drug delivery systems may reduce the frequency of dosing, and viral vectors have been employed to transfect cells that overexpress the coxsackie and adenovirus receptor (CAR), which facilitates the internalization of viral vectors loaded with therapeutic genes via receptor-mediated endocytosis [14]. In order to improve targeting for some aggressive bladder cancers, CAR expression would have to be increased, and this was shown using histone deacetylase inhibitors [15, 16]. Gene transfer can specifically target the mutated genome of bladder cancers [10, 17]. For instance, a replicating oncolytic adenovirus (CG0070) was engineered to destroy bladder cancer cells through a defect in the retinoblastoma pathway. This Phase I clinical trial showed that CG0070 had appreciable anti-tumor effect in 17 out of 35 patients (response rate 48.6%) [17]. However, a problem with viral-based vectors is their huge production costs, which limits their wide use. For instance, Glybera which was designed to treat lipoprotein lipase deficiency, a rare inherited disorder leading to severe pancreatitis, cost US $1 million per dose before being withdrawn from the market [18].

Non-viral vectors such as cationic polymers, which contain positively charged amine groups that can electrostatically bind with plasmids and siRNAs, are an attractive alternative gene transfer carrier. This is appealing as non-viral vectors are highly mucoadhesive, readily scalable, and have less immunogenicity, when compared with viral vectors [10, 19, 20]. Notably, PEI (polyethylenimine) is a frequently employed polymeric vector for gene transfer and has progressed to the clinical trial stage [20, 21]. In a Phase II clinical trial, 47 patients with recurrent NMIBC were given six intravesical instillations of PEI complexed with 20 mg BC-819 plasmid (an apoptosis gene) to suppress tumor growth and prevent recurrence [21]. The results showed that 33% of patients had complete tumor growth inhibition and 64% of patients had no recurrence at 3 months. It is worth noting that although the authors suggested that some patients experienced mild symptoms during this trial, 35 of 47 patients (74.5%) had

adverse effects such as dysuria, hematuria and urinary urgency. In a couple of preclinical evaluations, PEI exhibited appreciable cell toxicity regardless of whether its structure was linear, branched or derivatized [22-24]. One of the main reasons for a failure of another Phase II clinical trial was that the PEI-based delivery system encapsulating a human Interleukin-12 (IL-12) plasmid may have been too toxic for platinum-resistant ovarian cancer patients, with 20 patients experiencing adverse effects [25]. This suggests that the biocompatibility of the vectors will be one of the critical factors in determining the effectiveness of gene therapies for bladder cancer.

Herein, we have focused on chitosan and its derivatives, as non-viral vectors. Chitosan is a biopolymer derived from the naturally occurring chitin [26], and is more biocompatible than PEI [27]. In addition, it was suggested that the median lethal dose (LD_{50}) for chitosan in mice was 16 g per kg while that of NaCl was 3 g per kg [28], and chitosan could potentially be a material generally regarded as safe (GRAS) [27]. In the case of bladder gene delivery, we have shown in multiple studies the important role of chitosan in bladder gene delivery [29, 30]. Also, in a recent investigation, we demonstrated that adding glycol and ethylamino moieties to the chitosan produced the more water soluble [*N*-(2-ethylamino)-6-*O*-glycolchitosan] (EAGC) and resulted in higher gene binding affinity compared to unmodified chitosan, such that EAGC may be loaded with various nucleic acids (pDNA, siRNA, or mRNA) [31]. In this study, we evaluated how the chemistry of the polymer, especially the molecular weight of EAGC impacts intravesical gene delivery to the bladder. In order to achieve this, we opted to synthesize two different molecular weights of EAGC: (1) 40 – 50 kDa and (2) 80 – 90 kDa with a high ethylamino substitution (20 – 30%). Previously, it was shown that chitosan with these specific ranges of molecular weights either enhanced pDNA gene transfer or acted as a permeation enhancer for trans-epithelial drug delivery [32-34] and EAGC with 20 – 30% ethylamino substitution had a reasonable RNA transfection efficiency [31]. We also incorporated a "helper

lipid" DOPE (1,2-dioleoyl-sn-glycero-3-phosphoethanolamine) in our EAGC delivery system to produce a polymer-lipid hybrid system (EAGC-DOPE), as it has been demonstrated that DOPE-based non-viral vectors could facilitate gene transfer to the murine bladder with an efficiency up to a 100-fold higher than that shown by a viral vector [35]. In our studies, we demonstrate the importance of finely tuning the polymer molecular weight of EAGC to enable highly efficient localized gene delivery to the bladder.

2. Materials and methods

2.1 Materials

All chemicals and reagents were supplied by Sigma Aldrich unless otherwise specified. Visking seamless cellulose dialysis membranes were obtained from Medicell International Ltd., London, UK. DOPE lipid was purchased from Avanti Polar Lipids (Alabaster, USA). All chemicals and reagents were used without further purification. Cell culture reagents were purchased from Sigma Aldrich and Gibco unless otherwise indicated. Plasmids [pCMV·SPORT β-galactosidase (β-gal), 7853 bp, Invitrogen, UK; pCMV-GFP, 4479 bp, Addgene, USA; Firefly pCMV-Luc, 5566 bp, Addgene, USA] were propagated and isolated from DH5alpha bacteria using the Qiagen EndoFree plasmid Giga Kit (Qiagen, UK), following the manufacturer's instructions. The reconstituted aqueous plasmid solution was passed through a desalting Sephadex G25 column (GE Healthcare, UK) using deoxyribonuclease free water as the eluent. The plasmid was used immediately or stored at –50 °C for later use. siRNA against GP130 (siGP130) with the sequence: sense, 5'-CAGUAAAUCUCACAAAUGA-3', and a scrambled control (universal negative control#1), were purchased from Sigma-Aldrich, USA.

2.2 Methods

2.2.1 Synthesis of N-(2-ethylamino)-6-O-glycol chitosan (EAGC)

EAGC with similar ethylamino substitution and two different molecular weights was synthesized as described previously with modifications [31]. Briefly, two batches of GC (5 g each) were dissolved separately in hydrochloric acid (4 M, 96 mL) and placed for 45 min or 5 h in a preheated water bath at 50 °C, respectively. The product resulting from the acid degradation (GC45min or GC5h) was purified by dialysis (molecular weight cut off of dialysis membrane = 3500 Da) against deionized water (5 L) with six changes over 48 h. The dialyzed solution was freeze-dried, and GC45min or GC5h was recovered as a cream-colored cotton wool like material. The degraded GC (GC5h 200 mg, GC45min 100 mg) was dissolved separately in a solution of *N*-methyl-2-pyrrolidone (NMP) (40 mL for GC5h, 20 mL for GC45min) containing triethylamine in excess (1 mL for GC5h, 0.5 mL for GC45min). The solution was allowed to stir for 1 – 2 h at 40 °C in an oil bath until the GC was completely dissolved. To this dissolved GC was added 2-(*tert*-butoxycarbonylamino)ethyl bromide (7.39 g for GC5h or 3.695 g for GC45min). The reaction was left to stir for 24 h at 40 °C. Finally, the solution was mixed with water (40 mL) and washed with diethyl ether (3 x 50 mL) to remove the unreacted 2-(*tert*-butoxycarbonylamino)ethyl bromide. The aqueous phase was collected and dialyzed, as previously described, against deionized water (5L) with six changes over 24 h. The final polymer solution was freeze-dried. The recovered polymer was dissolved in HCl (50 mL, 4 M) and stirred for 4 h at room temperature in order to cleave the *tert*-butoxycarbonyl group. This solution was dialyzed as previously described and freeze dried to give *N*-(2-ethylamino)-6-*O*-glycol chitosan (EA25GC45 or EA28GC83) which presented as a cream colored solid.

2.2.2 Characterization of EAGC

The molecular weight of EAGC was measured using gel permeation chromatography with multi-angle laser light scattering (GPC–MALLS) as previously reported with modifications [31]. Briefly, the EAGC polymer was dissolved in a mixture of acetate buffer [0.04 M CH_3COONa (anhydrous)/0.2 M CH_3COOH, pH = 4.0] and methanol (35:65, v/v) to reach the desirable concentration (1 mg/mL). Then, EAGC solution was injected into a POLYSEP-GFC-P guard column (35 x 7.8 mm, Phenomenex, UK) attached to a POLYSEP-GFC-P 4000 column with an Agilent 1200 Series Autosampler connected to a Dawn® Multi-Angle Laser Light Scattering detector and an Optilab rEX Interferometric Refractometer (Wyatt Technology, USA). The EAGC solution was eluted with the mixture of acetate buffer and methanol as prepared for the polymer solution. For the refractive index measurements, various concentrations of EAGC were manually injected into Optilab rEX Interferometric Refractometer. The data were processed using Wyatt ASTRA software (Wyatt Technology, USA).

^{1}H NMR, was performed on EAGC in Deuterium Oxide (D_2O) on a Bruker AMX 500 MHz spectrometer (Bruker Instruments, UK). The ethylamino substitution was determined by comparing the ratio of the diethylamino substituted glycol chitosan with the sugar methine and methylene protons [31].

EA25GC45: Yield = 180 mg (90%), Mw = 44,850 Da, Mn = 43,690 Da, Mw/Mn = 1.027, dn/dc = 0.2255. ^{1}H-NMR: $\delta_{2.0}$ = ***CH_3***–CO– (acetyl-glycol chitosan), $\delta_{2.5}$ = –***CH***–N($CH_2CH_2NH_2$)$_2$ (C2 diethylamino-substituted glycol chitosan), $\delta_{2.9-3.1}$ = –***CH***–NH_2 (C2 glycol chitosan), $\delta_{3.1-3.2}$ = –CH–N(***CH_2CH_2***NH_2)$_2$ (diethylamino), $\delta_{3.4-4.2}$ = –***CH***–O– and –***CH_2***–OH– (glycol chitosan), $\delta_{4.5}$ = –***CH***–O– (C1 glycol chitosan).

EA28GC83: Yield = 85.7 mg (86%), Mw = 83,170 Da, Mn = 81,800 Da, Mw/Mn = 1.016, dn/dc = 0.1683. ^{1}H-NMR: $\delta_{2.0}$ = ***CH₃***–CO– (acetyl-glycol chitosan), $\delta_{2.5}$ = –***CH***–N(CH$_2$CH$_2$NH$_2$)$_2$ (C2 diethylamino-substituted glycol chitosan), $\delta_{2.9-3.1}$ = –***CH***–NH$_2$ (C2 glycol chitosan), $\delta_{3.1-3.2}$ = –CH–N(***CH₂CH₂***NH$_2$)$_2$ (diethylamino), $\delta_{3.4-4.4}$ = –***CH***–O– and –***CH₂***–OH– (glycol chitosan), $\delta_{4.5}$ = –***CH***–O– (C1 glycol chitosan).

2.2.3 Preparation of EACG-DOPE hybrid lipid nanoparticles (EGCDNPs) and complexation with plasmid DNA (pDNA) or siRNA

DOPE lipid (2 mg) dissolved in chloroform (1 mL) was placed in a round bottom flask and the solvent removed by rotary evaporation under reduced pressure for 20 min or even longer to form a thin lipid film. To the thin lipid film was added EAGC solution [1 mL, 2 mg/mL in 2 mM, pH = 6 phosphate buffer (PB)] and the whole flask containing EAGC and DOPE lipid was subjected to vigorous vortexing until a homogenous solution was achieved, yielding EAGC-DOPE lipid hybrid nanoparticles (EGCDNPs). The various EAGC polymers were named using the following nomenclature: GC (MW in kDa) EA (Mole% ethylamino) and thus a polymer with molecular weight of 45 kDa and containing 25 mole% ethylamino would be named: EA25GC45 and incorporation with DOPE lipid will lead to E25GC45DNPs. Plasmid DNA (β-gal, GFP and FLuc) or siGP130 dissolved in DNase/RNase free water was complexed with EGCDNPs in 2 mM, phosphate buffer (pH = 6) for 75 mins to produce polylipoplexes. The EGCDNPs solution typically contains 2 mg of EAGC and 2 mg of DOPE lipid in 1 mL phosphate buffer (2 mM, pH = 6) and was used as a single mass.

2.2.4 Physicochemical characterization of EGCDNPs

siRNA/plasmid DNA – NPs were characterized by assessing their size, surface charge, and morphology. Sizes were measured by Dynamic Light Scattering (Malvern, Nano ZS, UK)

using a He-Ne laser at 633 nm of wavelength. The zeta potential of the NPs was measured using a Zetasizer Nano ZS (Malvern, UK) in a folded capillary (0.75 mL) cuvette. Standard-latex beads (polystyrene, mean size: 200 nm) as well as zeta potential standard-polystyrene with a defined zeta potential ($-$ 42 $\pm$ 4.2 mV) were utilized to assess the accuracy of the instruments. For TEM, NPs placed onto a Carbon/Formvar grid (Agar Scientific, Stansted, UK) were stained with 1% uranyl acetate and imaged using a JEOL 1400 Plus microscope (JEOL Ltd., Japan).

2.2.5 Cell culture

Human invasive bladder cancer cells (UM-UC-3 and TCC-SUP), human prostate cancer cells (PC-3), and human glioblastoma cells (U87-MG) were purchased from American Type Culture Collection (ATCC, USA), and human embryonic kidney cells (HEK-293T) were a gift from Dr. Ahmed A. Ahmed (UCL School of Pharmacy). The derived drug-resistant UM-UC-3 (UM-UC-3R) cells were established by continuous exposure to gemcitabine and cisplatin [36]. UM-UC-3, UM-UC-3R, and TCC-SUP cell lines were cultured in MEME (Minimum Essential Medium Eagle), supplemented with FBS (10% v/v) and glutamine (1% v/v). PC-3 was cultured in F-12K medium (ATCC, USA), supplemented with FBS (10% v/v) and glutamine (1% v/v). U87-MG and HEK-293T cell lines were cultured with MEME, supplemented with FBS (10% v/v), GlutaMAX (1% v/v), and sodium pyruvate solution (1% v/v, Lonza Biologics Inc., UK). All cell lines were maintained at 37 °C in a humidified atmosphere containing 5% CO_2, and were routinely tested for mycoplasma (MycoAlert™, Lonza Biologics Inc.).

2.2.6 Plasmid transfection and in vitro cytotoxicity

To evaluate EGCDNPs *in vitro* plasmid transfection for protein up-regulation, two reporter genes (GFP-pDNA and β-gal-pDNA) were loaded separately in EA25GC45. In brief, cells were seeded at a density of 2.5 – 5 x 10^4 (12-well plate) or 5 x 10^5 (6-well plate) cells per well.

Complexes consisting of EGCDNPs, GFP-pDNA (1.6 µg pDNA for wells in a 12-well plate; 4 µg pDNA for wells in a 6-well plate) at EGCDNPs, pDNA mass ratios of 10:1, 20:1, or 40:1 were applied and incubated for 4 or 6 h followed by a 48 or 72 h recovery phase prior to being imaged by fluorescence microscopy (EVOS XL core Cell Imaging System, Life Technologies, UK or AXIO Observer A1, ZEISS, Germany) in the case of GFP expression. Cells also were treated for 4 h followed by a 72 h recovery phase with E25GC45DNPs – β-gal-pDNA complexes at EGCDNPs, pDNA mass ratios of 20:1 or 30:1 in comparison with Lipofectamine 2000 (Lipo 2k), which was formulated with β-gal-pDNA (4 µg/well pDNA for wells in a 6-well plate) at a Lipo 2k and β-gal-pDNA mass ratio of 5:2 using the manufacturer instructions. The β-galactosidase gene expression was measured using the β-galactosidase Enzyme Assay System (Promega, USA).

To evaluate the *in vitro* cytotoxicity, cells (HEK-293T, U87-MG, UM-UC-3, TCC-SUP, PC-3, and UM-UC-3R) were seeded at a density of 5,000 cells/well in a 96-well plate and left to recover for 24 h for all cell lines except for 48 h for TCC-SUP cells before being incubated with various concentrations of E25GC45DNPs (112.5 µg/mL, 56.3 µg/mL, 28.125 µg/mL, 14.063 µg/mL, and 1.4063 µg/mL) or Lipo 2k (25.0 µg/mL, 12.5 µg/mL, 6.25 µg/mL, 3.125 µg/mL, and 0.3125 µg/mL) for 6 h. Afterwards, the cells were replenished with 100 µL of medium without drug followed by 48 or 72 h of recovery. Ten µL per well of WST-1 reagent was subsequently added to the cells incubated at 37 °C. Cell viability was calculated based on the absorbance recorded at 450 nm of the EGCDNPs/Lipo-treated cells in reference to the non-treated cell control.

2.2.7 Cellular uptake and intracellular trafficking

Cellular uptake and intracellular deposition of GFP plasmid (GFP-pDNA) delivery by EGCDNPs were evaluated quantitively by flow cytometry and qualitatively by confocal

microscopy. In brief, GFP-pDNA was labelled with a Cy5 labeling kit (Mirus Bio, Madison, WI, USA) as per manufacturer's instructions (labelling efficiency:170 base pairs per Cy5). Complexes of EGCDNPs – Cy5 tagged GFP-pDNA at an EGCDNPs, GFP-pDNA mass ratio of 40:1 were prepared as described elsewhere (2.2.3 section). Fifty thousand HEK-293T cells were seeded on coverslips before being placed in a 24 well plate. Then Cy5 labelled GFP-pDNA complexed with EGCDNPs (1 µg pDNA/well) was added and incubated for 4 h followed by washing several times to remove the unbound complex. Cells were either trypsinized and subjected to flow cytometry analysis (MACSQuant, Miltenyi Biotec, Germany) or fixed with freshly prepared paraformaldehyde (4% in PBS) and stained with CF®488A-phalloidin dye (Actin staining) (Biotium, USA) followed by a counterstain with Hoechst (Nuclei staining). The abovementioned coverslips also were mounted with SlowFade mounting medium (Invitrogen, UK) and analyzed on a confocal microscope (Zeiss LSM710, Germany).

For quantitative colocalization analysis between the Cy5 labelled-GFP pDNA (red) and the nuclei labelled with Hoechst (blue), a Pearson's colocalization coefficient was calculated for 10 individual cells using the ImageJ (National Institutes of Health, USA) with 'Just Another Co-localization' (JACoP) Plugin (https://imagej.nih.gov/ij/plugins/track/jacop.html) as reported previously [37]. A background correction was performed prior to analysis to eliminate system variability in the image background. A Pearson's colocalization coefficient of 1 means total colocalization whereas 0 indicates no colocalization.

2.2.8 Small interfering RNA transfection and western blotting

To determine GP130 protein downregulation by siGP130 – EGCDNPs, western blotting was used as previously described [36]. In brief, the bladder cancer cells were transfected with siGP130 or siSC (4 µg siRNA/well) using Lipofectamine RNAiMAX (Invitrogen) or EGCDNPs before the protein was extracted and quantified. In brief, cells were treated with

EGCDNPs complexes (80 µg EGCDNPs, 4 µg siGP130 or 4 µg scrambled siRNA per well) and in serum-free medium for 6 h, followed by replenishing the wells with serum full medium for 48 h. Cells were then lysed with radioimmunoprecipitation assay (RIPA) buffer supplemented with cOmplete™, mini, EDTA-free protease inhibitor cocktail, 1 mM phenylmethylsulfonyl fluoride, 2 µg/mL aprotinin protease inhibitor, and 1 mM sodium fluoride. Lipofectamine – RNAiMAX complexes (4 µg siGP130/well) were applied to the cells as per manufacturer's instructions. Protein lysates were quantified using the Bradford Protein Assay (Bio-Rad, Laboratories, Inc., CA, USA) before being separated on SDS–PAGE gels (4 – 15%) and transferred to PVDF membranes. Antibodies used included GP130 (NBP2-15776; Novus Biologicals, USA), γ-H2AX (p-Ser 139; Santa Cruz, USA), beta-actin (13E5; Cell Signaling, USA) and a chemiluminescence system was used to detect the protein signal. All samples were normalized to a housekeeping protein, and band density was determined using ImageJ software.

2.2.9 Mouse intravesical instillation

Eight-week-old Swiss Webster (CFW) female mice (23 – 27 g) were instilled twice for 1 h with either saline or EGCDNPs – FLuc-pDNA complexes at the EGCDNPs, pDNA mass ratio of 11:1 (a dose of 6.4 µg FLuc-pDNA per mouse) once a day over 48 h. Also, CFW female mice were treated for 1 h with a single instillation or two instillations of saline or EGCDNPs – FLuc-pDNA complexes at the EGCDNPs, pDNA mass ratio of 11:1 (a dose of 2.4 µg of FLuc-pDNA) and containing chloroquine (3.4 µg) once a day over 24 h or once a day over 48 h. After 24 or 48 h, the mice were administered filtered D-luciferin (150 mg/kg) by intraperitoneal injection. The mice were placed in the Xenogen IVIS Spectrum (PerkinElmer, USA) under 1 – 2% isoflurane. Living Image software (version 4.5.2) was used for image acquisition and

analysis. All animal studies were approved by the Institutional Animal Care and Use Committee of Yale University.

Mice were euthanized before the bladders and livers were removed. Organs were rinsed in PBS and flash frozen in liquid nitrogen. Tissues were homogenized with a pestle and mortar in liquid nitrogen. The tissues homogenates were lysed in 1X Reporter Lysis Buffer (Promega, USA), underwent one freeze-thaw cycle in liquid nitrogen and 37 °C incubation to enable the completion of lysis, and centrifuged at 12000 x g for 15 min at 4 °C. Supernatants were assayed for total protein content (Pierce^{TM} BCA Protein Assay kit, Thermo Scientific) and for luciferase content (BrightGlo and QuantiLum, Promega, USA).

2.2.10 Hematoxylin and eosin (H & E) and immunohistochemistry staining (IHC)

Paraffin-embedded mouse bladders were deparaffinized in xylene before being rehydrated with graded ethanol. All specimens were stained with H & E as described [38]. IHC was performed as previously published with modifications [39]. Briefly, heat-induced epitope retrieval was carried out in citrate buffer solution at 95 °C for 30 min. Endogenous peroxidase was blocked at room temperature before being incubated with primary antibodies at 4 °C overnight and secondary antibodies at room temperature for 1 h. Slides were then stained using 3,3'-diaminobenzidine (DAB) and counterstained with hematoxylin. Paraffin-embedded human UM-UC-3 cell pellets treated with EGCDNPs loaded with a luciferase plasmid, were used as a positive control for the luciferase staining.

2.2.11 Statistical analysis

GraphPad (Prism 7 software) was used to prepare all graphs and to perform one-way and two-way analysis of variance (ANOVA), two-tailed t-tests or Mann–Whitney tests. Mann–Whitney tests were performed for experiments for which the data were determined to be non-parametric

by the normality test (that is, firefly luciferase expression from harvested bladder and liver tissues). All experiments were performed in triplicate unless otherwise stated. Error bars indicate the standard deviation (SD). All statistical tests were considered to be statistically significant in which * represents $p < 0.05$, ** represents $p < 0.01$, *** represents $p < 0.001$, and **** represents $p < 0.0001$ unless indicated differently. For IC_{50} analysis, nonlinear fit-log (inhibitor) versus normalized response (variable slope) was performed as reported previously [40].

Results

3.1 Preparation and characterization of pDNA/siRNA – EGCDNPs.

Two distinct polymers were synthesized with different molecular weights and similar degrees of ethylamino substitutions: EA25GC45 (45 kDa, 25 mole substitution of ethylamino per 100 mole of GC monomer) and EA28GC83 (83 kDa, 28 mole substitution of ethylamino per 100 mole of GC monomer) (**Figure 1A**). A schematic diagram of the self-assembled EAGC-DOPE (1:1 mass ratio of EAGC to DOPE) hybrid nanoparticles (EGCDNPs) is shown in **Figure 1B**. Transmission electron microcopy (TEM) data (**Figure 1C**) confirmed the structure proposed in **Figure 1B** and the EGCDNPs (e.g. E25GC45DNPs) alone appear as 30 ± 13 nm nanoparticles with lipid cores (**Figures 1C–D**).

Prior to condensation, both naked siRNA and naked pDNA presented as electron dense fibers due to the staining of the hydrophilic regions in siRNA and pDNA (**Figures S1A–B**). When loaded with either GFP-pDNA at an EGCDNPs, pDNA mass ratio of 10:1 or with siGP130 at an EGCDNPs, siRNA mass ratio of 20:1, E25GC45DNPs complexes were slightly bigger in

diameter, with diameters of 98 ± 28 nm (siGP130) (**Figures S1C, E)** and 67 ± 15 nm (GFP-pDNA) (**Figures S1D, F**) compared a diameter of 30 ± 13 nm with E25GC45DNPs alone.

The DLS sizing data revealed that siGP130 – E25GC45DNPs were around 130 nm in diameter (**Figures 2A–B**). Similarly, the GFP-pDNA – E25GC45DNPs complexes were 115 nm in diameter (**Figures 2C**). The E28GC83DNPs complexes containing a higher molecular weight of EAGC produced significantly larger size particles in comparison with the E25GC45DNPs complexes (**Figure 2C**) (361 nm vs 115 nm, $p < 0.001$), inferring that the molecular weight of EAGC played a role in regulating complex size formation. This result is in agreement with our previous report that molecular weight has a direct correlation with polymeric vesicle size [41]. Additionally, E28GC83DNPs when encapsulating another type of pDNA (FLuc-pDNA) at an EGCDNPs, pDNA mass ratio of 10:1 presented as 204 nm NPs (**Figure 2D**).

Zeta potential data revealed that when electrostatic binding of anionic GFP-pDNA with EGCDNPs at an EGCDNPs, pDNA mass ratio of 10:1 occurred, the complexes were positively charged (+ 22.2 ± 0.8 mV for E25GC45DNPs; + 19.2 ± 1.0 mV for E28GC83DNPs) due to excess of the positively charged protonated amines arising from the EAGC polymer (**Figure 2C**). Also, E25GC45DNPs – siGP130 complexes formulated at an EGCDNPs, siRNA mass ratio of 20:1 displayed a zeta potential of + 21.0 ± 0.2 mV (**Figure 2A**). Furthermore, E28GC83DNPs – FLuc-pDNA complexes also exhibited an overall positive charge with a zeta potential of + 23.2 ± 2.1 mV (**Figure 2D**).

3.2 EAGC-DOPE lipid hybrid nanoparticles (EGCDNPs) exhibit a superior biocompatibility profile and are efficient plasmid DNA transfection agents.

We first set out to evaluate whether the addition of DOPE lipid could in principle lead to more efficient gene transfer. We tested the efficiency of 45 kDa EAGC as an *in vitro* gene transfection agent and compared it with E25GC45DNPs. Utilizing GFP-pDNA as a reporter gene and a fluorescence microscope, we showed that E25GC45DNPs significantly enhanced GFP expression in bladder cancer cells (UM-UC-3), when compared with EAGC-induced transfection (**Figures S2A–B**). We quantitively demonstrated, in hard-to-transfect glioma cells (U87-MG), that GFP-pDNA formulated at EGCDNPs, GFP-pDNA mass ratios of 20:1, 30:1, and 40:1 resulted in a higher GFP percentage of positive cells than the GFP-pDNA – EAGC treated groups ($23.2 \pm 2.2\%$ vs $11.9 \pm 3.5\%$, $p < 0.05$; $27.7 \pm 2.3\%$ vs $15.0 \pm 3.3\%$, $p < 0.01$; $26.8 \pm 5.0\%$ vs $17.0 \pm 3.6\%$, $p < 0.05$, respectively) (**Figures S2C**). To further investigate whether this vector could induce GFP-pDNA transfer in a wide range of cell lines, which may pave the way for the development of new therapies for various medical indications, we tested the transfection efficiency of GFP-pDNA – E25GC45DNPs in HEK-293T human embryonic kidney cells, U87-MG glioma cells, UM-UC-3 and TCC-SUP bladder cancer cells, UM-UC-3R chemo-resistant bladder cancer cells, and PC-3 prostate cancer cells. It was noted (**Figure 3A)** that all cells emitted green fluorescence after the introduction of the exogenous GFP plasmid by E25GC45DNPs indicative of successful transfection.

To validate our finding, the commercial transfection reagent – Lipofectamine 2000 (Lipo 2k) was used as a positive control and another reporter gene (β-gal-pDNA) was applied to the HEK-293T cells using E25GC45DNPs and Lipo 2k as transfection reagents. The transfection results indicated that E25GC45DNPs complexes (EGCDNPs, pDNA mass ratios = 20:1 or 30:1) produced a lower amount of β-gal-pDNA expression in HEK-293T cells than the Lipo 2k – β-gal-pDNA formulated at a lipid, pDNA mass ratio of 5:2 (35 ± 1 mU vs 140 ± 24 mU, $p < 0.0001$; 38 ± 2 mU vs 140 ± 24 mU, $p < 0.0001$, respectively) (**Figure 3B**). However, cytotoxicity assessed by the WST-1 assay showed that the E25GC45DNPs were more

biocompatible gene transfection reagents than the Lipo 2k. 90 – 99% of cells were determined viable with EGCDNPs at the IC_{50} (half maximal inhibitory concentration) of Lipo 2k in six tested cell lines (**Figure 4** and **Table S1**). Interestingly, it seems that Lipo 2k showed a clear cell type-dependent cytotoxicity profile, with prostate cancer cells (PC-3) showing the least toxicity towards Lipo 2k (IC_{50} of 22.22 ± 5.78 μg/mL), followed by glioma cells (U87-MG, IC_{50} of 7.27 ± 0.78 μg/mL). Bladder cancer cells including UM-UC-3 (IC_{50} of 3.71 ± 1.40 μg/mL), UM-UC-3R (IC_{50} of 2.51 ± 0.76 μg/mL), and TCC-SUP (IC_{50} of 1.20 ± 0.86 μg/mL) and HEK-293T human embryonic kidney cells (IC_{50} of 1.32 ± 0.43 μg/mL) showed a similar sensitivity to the Lipo 2k treatment (**Table S1**).

3.3 EGCDNPs-enabled pDNA transfection in vitro was due to the enhanced pDNA cellular uptake resulting in pDNA accumulating at the perinuclear and nuclear regions.

To understand the mechanism of transfection by E25GC45DNPs, flow cytometry and confocal microscopy were utilized in HEK-293T cells. After 4 h of transfection with Cy5-labelled GFP-pDNA – E25GC45DNPs, there were 29.61 ± 1.96% of Cy5 positive cells compared to 0.32 ± 0.03% of untreated cells being Cy5 positive ($p < 0.0001$) (**Figures S3A–B**). We also presented a non-invasive approach to evaluate cell uptake that is involved with slicing confocal images into 8 slices (2.2 μm distance between slices) and staining cell nuclei with blue (Hoechst) and actin with green (CF®488A-phalloidin), respectively. As the white arrows indicate (**Figure 5**), the particles of Cy5-labelled GFP-pDNA (red) delivered by E25GC45DNPs colocalize with the nuclear stain in the same focal plane. This indicates the accumulation of pDNA in the perinuclear and nuclear regions of the cell. Furthermore, the quantitative analysis confirmed a partial correlation between the Cy5-labelled GFP-pDNA and the Hoechst-stained nuclei with a Pearson's correlation coefficient of 0.33 ± 0.14 (**Figure 5**).

19

3.4 EGCDNPs complexed with siGP130 were as efficacious as Lipofectamine RNAiMAX siGP130 in silencing GP130 protein while inducing less DNA damage in bladder cancer cell lines.

We set out to examine the ability of E25GC45DNPs to deliver siRNA targeting GP130 in UM-UC-3 and UM-UC-3R bladder cancer cells. GP130 protein was chosen as previous studies demonstrated that GP130, a signal transducer for interlukin-6 (IL-6), was highly expressed in aggressive bladder cancers [29] and the silencing of GP130 could reduce bladder cancer cell viability and migration [36]. The data in **Figure 6** show that siGP130 formulated with E25GC45DNPs, and applied at 4 μg/well caused specific downregulation of GP130 protein in UM-UC-3 and UM-UC-3R cells, when compared to the application of scrambled siRNA ($p < 0.05$ and $p < 0.01$, respectively) (**Figures 6A–B and D**). The knockdown efficiency in UM-UC-3R cells was comparable to the Lipofectamine RNAiMAX – siGP130 treated group (**Figure 6D**, no significant difference was observed). Although the efficiency of silencing GP130 achieved by E25GC45DNPs siRNA in UM-UC-3 cells was inferior to siGP130 complexing with Lipofectamine RNAiMAX ($p < 0.01$), siGP130 formulated with E25GC45DNPs produced considerably less Gamma-H2AX (γ-H2AX) than siGP130 complexed with Lipofectamine RNAiMAX ($p < 0.01$) (**Figures 6A–C**). This reduced γ-H2AX expression after the treatment of E25GC45DNPs complexes when compared to lipoplexes treatment also was observed in UM-UC-3R cells ($p < 0.01$) (**Figure 6E**).

3.5 EGCDNPs comprising of higher molecular weight EAGC (83 kDa) were the most active firefly luciferase plasmid (FLuc-pDNA) delivery vectors in the healthy murine bladder.

To evaluate whether EGCDNPs could be active in gene transfer to the *in vivo* bladder, we chose two EGCDNPs: E25GC45DNPs and E28GC83DNPs with similar ethylamino

substitutions (25% mole substitution and 28% mole substitution, respectively) for EACG but with different molecular weights (45 kDa vs 83 kDa). Furthermore, since the BPB is known to be one of the most efficient biological barriers in mammalian tissues [42], we also attempted to determine if the gene transfer across the BPB could be augmented by an endosomolytic agent – chloroquine, that could buffer the endosome and promote gene release from the endosome to achieve efficient cellular uptake [43]. With the aid of chloroquine, E28GC83DNPs complexes, containing a higher molecular weight of EAGC (83 kDa), produced higher levels of firefly luciferase expression in a healthy murine bladder than the E25GC45DNPs complexes containing a lower molecular weight of EAGC (45 kDa) 24 h after transfection (**Figure S4A**). However, we did not observe any transfection after 48 h when we instilled the E28GC83DNPs gene complexes twice in the presence of chloroquine. These results indicate that chloroquine was not necessary for inducing gene transfer in the bladder (**Figure S4B**).

Even when gene transfer conditions were optimum, E25GC45DNPs were still unable to efficiently deliver FLuc-pDNA to the bladder and cross the BPB to produce exogenous luciferase expression (**Figure 7A, C**). However, optimization of E28GC83DNPs – FLuc-pDNA complexes, at an EGCDNPs, pDNA mass ratio of 11:1 (6.4 µg pDNA per instillation) provided the best and most reproducible conditions for inducing significantly higher gene transfer in the *in vivo* murine bladder than saline controls (**Figures 7B, D**) ($p < 0.05$). In total, 12.8 µg of FLuc-pDNA could be delivered to the murine bladder using E28GC83DNPs. The differentiated gene transfer profiles for E25GC45DNPs and E28GC83DNPs indicate that the molecular weight of EAGC is a strong driver for efficient gene transfection in *in vivo* murine bladder models. Additionally, the bioluminescence obtained from the IVIS spectrum after transfection of FLuc-pDNA to the murine bladder by the E28GC83DNPs correlated well with the extraction and quantification of FLuc protein from harvested bladder tissues treated with

FLuc-pDNA formulated with E28GC83DNPs (**Figure 7E**) (saline vs treatment: 0.12 ± 0.15 vs 1.35 ± 1.81 ng/g, $p < 0.05$). There was no measurable distribution of exogenous firefly luciferase in the liver, indicating that the bladder was the prime accumulation site for the complexes of E28GC83DNPs – FLuc-pDNA (**Figure 7F**). The observed luciferase expression in the bladder was attributed to the fact that the E28GC83DNPs could efficiently penetrate the BPB and facilitate the uptake of FLuc-pDNA to the lamina propria (**Figures 8A–B**).

To evaluate the *in vivo* side effects following the administration of E28GC83DNPs complexes at various doses, the murine bladders were collected two days after the last instillation. The bladders were sectioned and stained with H & E. No significant difference in the infiltration of neutrophils or lymphocytes was observed between the saline and E28GC83DNPs – FLuc-pDNA treatment groups. The intact bladder epithelium was well preserved (**Figure 9A**). Acetic acid-treated positive controls showed intense staining for myeloperoxidase (MPO), whereas, the saline and E28GC83DNPs – FLuc-pDNA treated bladders showed little or no MPO staining, indicating that no appreciable inflammation was produced by the NPs (**Figures 9B–C**).

4. Discussion

One of the major obstacles to efficient delivery of therapeutic agents to the bladder tissue involves penetration of the BPB. To enhance drug penetration urothelial cell desquamation agents such as ethylendiamintetraacetate (EDTA) [44], lipopolysaccharide (endotoxin) [45], and electromotive devices [46] have been used. Mitomycin C is a commonly used intravesical chemotherapeutic agent for treating superficial bladder cancer [46]. An electromotive device was designed and used to facilitate the intravesical delivery of mitomycin C. Despite these

promising results, the use of electromotive devices has been slow to be adopted in the US making the transition into the clinic challenging [46, 47].

Gene-based therapeutics have had some success for various diseases including head and neck squamous cell carcinoma, hereditary blindness, and hereditary transthyretin amyloidosis with polyneuropathy [48-50]. However, there have been some safety concerns using viral vectors as well as the high costs [18, 51, 52] associated with treatment. Currently, there remains no gene-based therapeutics for the treatment of bladder diseases. This likely is attributed to the lack of an effective, biocompatible gene delivery system. The focus of the present study was to address this unmet challenge by developing an efficient gene delivery system that would provide localized gene delivery to the bladder while avoiding systemic toxicity.

Polymeric nanoparticles (NPs) have been advocated as promising intravesical drug delivery systems. Chitosan, a mucoadhesive polysaccharide derived from the exoskeletons of crustaceans, was shown to facilitate intravesical drug delivery as a result of its high viscosity, which reduced loss from voiding [53, 54]. Previously, we showed the pivotal role that intratumoral injections of chitosan and its derivatives played in shrinking tumor growth in a xenograft bladder cancer model using a GP130 siRNA and a survivin siRNA [29, 30]. In addition, these particles facilitated urothelial penetration when intravesically instilled and enhanced the transfection of siRNAs into human bladder cancer cells [29, 30]. Herein, we focused on enhancing localized delivery to the bladder. We devised a robust self-assembled approach by adding DOPE (1,2-dioleoyl-sn-glycero-3-phosphoethanolamine) lipid to EAGC in a 1:1 mass ratio to yield EACG-DOPE lipid hybrid nanoparticles (EGCDNPs).

In constructing EGCDNPs, we focused mainly on the polymer molecular weight. Some reports have noted that EGCDNPs with a high molecular weight (213 kDa, with a degree of deacetylation of 88%) showed a high zeta potential (+ 23 mV), improved cellular uptake, and

exhibited excellent transfection efficiency [55]. Conversely, other reports have suggested that 40 and 84 kDa chitosan demonstrated higher levels of luciferase expression in SOJ cells, while the 1 kDa chitosan counterpart, presumably owing to a very limited number of positively charged amine groups, resulted in no transfection response [56]. Nonetheless, we have shown that the molecular weight of chitosan derivatives was the overriding factor for controlling its transfection efficiency. This was irrespective of its surface modification, including the addition of palmitoyl or quaternary ammonium groups [57]. Moreover, it is tempting to assume that a higher molecular weight (over 100 kDa) chitosan may be able to carry a relatively large number of protonable amines, which might disrupt the negative charged cell membrane, making it less biocompatible [58]. We have evaluated the feasibility of balancing amine density and molecular weight to effect gene transfer. We demonstrated that a 45 kDa chitosan derivative EAGC, with 25% mole ethylamino substitution, when added to DOPE (E25GC45DNPs), led to a significantly higher level of GFP-pDNA transfection than EAGC-treated groups using UM-UC-3 and U87-MG cell lines (**Figure S2**), indicating that the incorporation of the DOPE lipid gave rise to improved gene transfer. Furthermore, E25GC45DNPs were able to transfect GFP-pDNA in six tested cell lines, suggesting its potential for the development of new therapies. There are several possible mechanisms for DOPE-assisted nucleic acid cellular transfer. First, DOPE lipid has a conical structure, which promotes nanoparticle fusion to the cell membrane, enabling DNA transfer [59]. The subsequent phase transition into a hexagonal structure leads to the rupture of endosome such that pDNA is released into the cytosol. Then the released pDNA is assisted by DOPE lipid to be trafficked rapidly into the nucleus [60]. Second, it is possible that the observed E25GC45DNPs-induced gene transfer is related to its overall positive charge when loaded with GFP-pDNA (+ 22.2 ± 0.8 mV) and to its spherical nanoparticle shape and relatively small size (115 nm) (**Figure 2C**). Last, we showed that there is a significant cellular uptake of GFP-pDNA facilitated by E25GC45DNPs in HEK-293T cells

(**Figure S3B**). Z-stack images showed that after 4 h of treatment, GFP-pDNA complexed with E25GC45DNPs was trafficked intracellularly, leading to perinuclear and nuclear accumulation (**Figure 5).**

When we compared the transfection efficiency of E25GC45DNPs in delivering β-gal-pDNA with the commercial transfection reagent, Lipofectamine 2000 (Lipo 2k), E25GC45DNPs were 30% as efficient as Lipo 2k. However, the WST-1 assay (**Figure 4** and **Table S1)** revealed that the E25GC45DNPs were significantly less toxic than the commercial transfection reagent – Lipo 2k, as virtually no toxicity was seen with the EGCDNPs at up to 112.5 µg/mL in all but the HEK-293T cell line, whereas some cytotoxicity was seen at an EGCDNPs concentration above 112.5 µg/mL.

In transfecting another type of nucleic acid – a small interference RNA (siRNA), Lipofectamine RNAiMAX loaded with siGP130 was able to specifically silence the GP130 protein, but with high cytotoxicity as was shown by upregulation of Gamma-H2AX (γ-H2AX), a DNA damage marker in UM-UC-3 and UM-UC-3R cells (**Figures 6A, C and E**). Also, we showed that when siGP130 was complexed with E25GC45DNPs, it could knockdown GP130 protein in UM-UC-3R cells to a similar extent as did Lipofectamine RNAiMAX-mediated treatments (**Figures 6A, D**). However, it produced less γ-H2AX in both UM-UC-3 and UM-UC-3R cells than Lipofectamine RNAiMAX (**Figures 6A, C and E**). The specific downregulation of the GP130 protein by siGP130 – E25GC45DNPs is in agreement with our previous findings using chitosan functionalized nanoparticles in *in vitro* and *in vivo* xenograft models [29].

Having established the efficacy and biocompatibility profile of EGCDNPs, we set out to evaluate whether EGCDNPs could be effective for gene transfer in the bladder. The intravesical instillation of E25GC45DNPs containing pDNA encoding Firefly luciferase (FLuc-pDNA)

(6.4 µg per instillation) did not produce enough exogenous luciferase expression in the healthy murine bladder to make it distinguishable from the saline-control group (**Figures 7A, C**), whereas higher molecular weight of EAGC (83 kDa, with 28% ethylamino mole substitution) incorporated with DOPE lipid (E28GC83DNPs) could facilitate a significant number of FLuc-pDNA cellular transfers, inferring that the molecular weight of EGCDNPs could play a pivotal role in regulating luciferase expression in the bladder (**Figures 7B, D**).

Our goal with this investigation was to clarify the relationship between molecular weight and transfection of chitosan derivatives. Kolawole et al. suggested that among various molecular weights of chitosan (62, 124 and 370 kDa), the 370 kDa (chitosan) (NPs) displayed superior resistance to urine washes, supporting its use as a mucoadhesive gene delivery vector to the bladder [54]. However, the syringeability (i.e., the ability for the treatment to pass from the syringe to the bladder) of the higher molecular weight chitosan (124 and 370 kDa) was significantly lower than that of the 62 kDa chitosan, indicating that 62 kDa chitosan may be the most suitable formulation for intravesical instillation *in vivo* [54]. Our results are in agreement with those of Hsu and coworkers who showed that 80 kDa chitosan could bind to the negatively-charged integrin $\alpha_V\beta_3$ present in epithelial enterocytes (Caco-2 cells), leading to the temporary disruption of the tight junctions, and ultimately enhancing absorption of the macromolecules [33]. To understand if there was any potential accumulation of E28GC83DNPs systemically, we quantified the luciferase expression in the liver, which is the major metabolic site of nanoparticles entering the blood stream. E28GC83DNPs complexes had no luciferase expression in the liver when compared with the saline groups (**Figure 7F**). H & E and IHC studies showed that E28GC83DNP complexes had minimal impact on the morphology of normal bladder cells with no appreciable inflammatory response according to MPO expression. Due to the robust transfection efficiency of EGCDNPs, as little as 12.8 µg of

FLuc-pDNA can be delivered to induce firefly luciferase expression in the intact urothelium, drastically reducing the likelihood of any potential toxic effects.

Yu et al. devised an efficient transfection technique using electroporation to deliver GFP-pDNA to the bladder [61]. However, the invasive nature of this technique and the incorporation of electric pulses will make this approach less appealing and more challenging to translate from the bench to the clinic, especially since a skilled operator would be required [61]. Furthermore, they recommended a minimum dose of 20 µg to elicit a transfection response; however, electroporation at this dose still induced GFP expression only in the bladder urothelium. Similarly, Horie and co-authors used ultrasound with nanobubbles to transfect luciferase plasmid DNA to the bladder wall of BALB/c mice [62]. The authors showed that a higher luciferase expression in the murine bladder was achieved when using 33 µg pDNA under adequate external acoustic energy. However, ultrasound with nanobubbles could only deliver pDNA in a certain area of the bladder, which limited its applicability in treating bladder cancer, due to the fact that one-third of bladder cancer patients spontaneously form tumors at multiple locations within the bladder [63]. We showed that FLuc-pDNA formulated with E28GC83DNPs can still be effective at a dose as little as 12.8 µg. Furthermore, E28GC83DNPs – FLuc-pDNA complexes led to a wide expression of firefly luciferase in the urothelium, and some of complexes even penetrated into lamina propria.

Herein, we developed a positively charged EAGC-DOPE hybrid system that was efficient and less toxic compared to the commercial transfection reagent, Lipofectamine, in mediating gene transfer. We showed, for the first time, that the EAGC-DOPE hybrid system, formulated with a high molecular weight component of EAGC was more able in transfecting in an *in vivo* normal murine bladder model.

Declaration of competing interest

There is no competing interest to report.

Author contributions

Ijeoma F. Uchegbu, Darryl T. Martin, Robert M. Weiss, and Andreas G. Schätzlein conceived and designed the experiments. Gang Li and Shanshan He wrote the manuscript. Gang Li, Shanshan He, and Darryl T. Martin performed the experiments and analyzed the data. All authors reviewed the manuscript prior to publication.

6. References

[1] A. Richters, K.K.H. Aben, L. Kiemeney, The global burden of urinary bladder cancer: an update, World J Urol, 38 (2020) 1895-1904.

[2] F. Bray, J. Ferlay, I. Soerjomataram, R.L. Siegel, L.A. Torre, A. Jemal, Global cancer statistics 2018: GLOBOCAN estimates of incidence and mortality worldwide for 36 cancers in 185 countries, CA Cancer J Clin, 68 (2018) 394-424.

[3] R.L. Siegel, K.D. Miller, A. Jemal, Cancer statistics, 2020, CA Cancer J Clin, 70 (2020) 7-30.

[4] S.R. Krishna, B.R. Konety, Current Concepts in the Management of Muscle Invasive Bladder Cancer, Indian J Surg Oncol, 8 (2017) 74-81.

[5] C. Yeung, T. Dinh, J. Lee, The health economics of bladder cancer: an updated review of the published literature, Pharmacoeconomics, 32 (2014) 1093-1104.

[6] J.J. Ahn, R.A. Ghandour, J.M. McKiernan, New agents for bacillus Calmette-Guerin-refractory nonmuscle invasive bladder cancer, Curr Opin Urol, 24 (2014) 540-545.

[7] V.T. Packiam, S.C. Johnson, G.D. Steinberg, Non-muscle-invasive bladder cancer: Intravesical treatments beyond Bacille Calmette-Guerin, Cancer, 123 (2017) 390-400.

[8] J. Bosschieter, J.A. Nieuwenhuijzen, T. van Ginkel, A.N. Vis, B. Witte, D. Newling, G.M.A. Beckers, R.J.A. van Moorselaar, Value of an Immediate Intravesical Instillation of Mitomycin C in Patients with Non-muscle-invasive Bladder Cancer: A Prospective Multicentre Randomised Study in 2243 patients, Eur Urol, 73 (2018) 226-232.

[9] E.M. Messing, C.M. Tangen, S.P. Lerner, D.M. Sahasrabudhe, T.M. Koppie, D.P. Wood, Jr., P.C. Mack, R.S. Svatek, C.P. Evans, K.S. Hafez, D.J. Culkin, T.C. Brand, L.I. Karsh, J.M. Holzbeierlein, S.S. Wilson, G. Wu, M. Plets, N.J. Vogelzang, I.M. Thompson, Jr., Effect of Intravesical Instillation of Gemcitabine vs Saline Immediately Following Resection of Suspected Low-Grade Non-Muscle-Invasive Bladder Cancer on Tumor Recurrence: SWOG S0337 Randomized Clinical Trial, JAMA, 319 (2018) 1880-1888.

[10] S. GuhaSarkar, R. Banerjee, Intravesical drug delivery: Challenges, current status, opportunities and novel strategies, J Control Release, 148 (2010) 147-159.

[11] L. Denis, Anaphylactic reactions to repeated intravesical instillation with cisplatin, Lancet, 1 (1983) 1378-1379.

[12] M. Kates, A. Date, T. Yoshida, U. Afzal, P. Kanvinde, T. Babu, N.A. Sopko, H. Matsui, N.M. Hahn, D.J. McConkey, A. Baras, J. Hanes, L. Ensign, T.J. Bivalacqua, Preclinical Evaluation of Intravesical Cisplatin Nanoparticles for Non-Muscle-Invasive Bladder Cancer, Clin Cancer Res, 23 (2017) 6592-6601.

[13] S. Lu, L. Xu, E.T. Kang, R. Mahendran, E. Chiong, K.G. Neoh, Co-delivery of peptide-modified cisplatin and doxorubicin via mucoadhesive nanocapsules for potential synergistic intravesical chemotherapy of non-muscle-invasive bladder cancer, Eur J Pharm Sci, 84 (2016) 103-115.

[14] H. Su, H. Jiang, T. Tao, X. Kang, X. Zhang, D. Kang, S. Li, C. Li, H. Wang, Z. Yang, J. Zhang, C. Li, Hope and challenge: Precision medicine in bladder cancer, Cancer Med, 8 (2019) 1806-1816.

[15] M.D. Sachs, M. Ramamurthy, H. Poel, T.J. Wickham, M. Lamfers, W. Gerritsen, W. Chowdhury, Y. Li, M.P. Schoenberg, R. Rodriguez, Histone deacetylase inhibitors upregulate expression of the coxsackie adenovirus receptor (CAR) preferentially in bladder cancer cells, Cancer Gene Ther, 11 (2004) 477-486.

[16] T. Okegawa, K. Nutahara, R.C. Pong, E. Higashihara, J.T. Hsieh, Enhanced transgene expression in urothelial cancer gene therapy with histone deacetylase inhibitor, J Urol, 174 (2005) 747-752.

[17] J.M. Burke, D.L. Lamm, M.V. Meng, J.J. Nemunaitis, J.J. Stephenson, J.C. Arseneau, J. Aimi, S. Lerner, A.W. Yeung, T. Kazarian, D.J. Maslyar, J.M. McKiernan, A first in human phase 1 study of CG0070, a GM-CSF expressing oncolytic adenovirus, for the treatment of nonmuscle invasive bladder cancer, J Urol, 188 (2012) 2391-2397.

[18] M. Senior, After Glybera's withdrawal, what's next for gene therapy?, Nat Biotechnol, 35 (2017) 491-492.

[19] H. Yin, R.L. Kanasty, A.A. Eltoukhy, A.J. Vegas, J.R. Dorkin, D.G. Anderson, Non-viral vectors for gene-based therapy, Nat Rev Genet, 15 (2014) 541-555.

[20] Y. Yue, C. Wu, Progress and perspectives in developing polymeric vectors for in vitro gene delivery, Biomater Sci, 1 (2013) 152-170.

[21] O.N. Gofrit, S. Benjamin, S. Halachmi, I. Leibovitch, Z. Dotan, D.L. Lamm, N. Ehrlich, V. Yutkin, M. Ben-Am, A. Hochberg, DNA based therapy with diphtheria toxin-A BC-819: a phase 2b marker lesion trial in patients with intermediate risk nonmuscle invasive bladder cancer, J Urol, 191 (2014) 1697-1702.

[22] A. Brownlie, I.F. Uchegbu, A.G. Schatzlein, PEI-based vesicle-polymer hybrid gene delivery system with improved biocompatibility, Int J Pharm, 274 (2004) 41-52.

[23] W.P. Cheng, A.I. Gray, L. Tetley, B. Hang Tle, A.G. Schätzlein, I.F. Uchegbu, Polyelectrolyte nanoparticles with high drug loading enhance the oral uptake of hydrophobic compounds, Biomacromolecules, 7 (2006) 1509-1520.

[24] V. Kafil, Y. Omidi, Cytotoxic impacts of linear and branched polyethylenimine nanostructures in a431 cells, BioImpacts, 1 (2011) 23-30.

[25] R.D. Alvarez, M.W. Sill, S.A. Davidson, C.Y. Muller, D.P. Bender, R.L. DeBernardo, K. Behbakht, W.K. Huh, A phase II trial of intraperitoneal EGEN-001, an IL-12 plasmid formulated with PEG-PEI-cholesterol lipopolymer in the treatment of persistent or recurrent epithelial ovarian, fallopian tube or primary peritoneal cancer: a gynecologic oncology group study, Gynecol Oncol, 133 (2014) 433-438.

[26] M.D. Buschmann, A. Merzouki, M. Lavertu, M. Thibault, M. Jean, V. Darras, Chitosans for delivery of nucleic acids, Adv Drug Deliv Rev, 65 (2013) 1234-1270.

[27] T. Kean, M. Thanou, Biodegradation, biodistribution and toxicity of chitosan, Adv Drug Deliv Rev, 62 (2010) 3-11.

[28] A.S. Kritchenkov, S. Andranovits, Y.A. Skorik, Chitosan and its derivatives: vectors in gene therapy, Russian Chemical Reviews, 86 (2017) 231-239.

[29] D.T. Martin, H. Shen, J.M. Steinbach-Rankins, X. Zhu, K.K. Johnson, J. Syed, W.M. Saltzman, R.M. Weiss, Glycoprotein-130 Expression Is Associated with Aggressive Bladder Cancer and Is a Potential Therapeutic Target, Mol Cancer Ther, 18 (2019) 413-420.

[30] D.T. Martin, J.M. Steinbach, J. Liu, S. Shimizu, H.Z. Kaimakliotis, M.A. Wheeler, A.B. Hittelman, W. Mark Saltzman, R.M. Weiss, Surface-modified nanoparticles enhance transurothelial penetration and delivery of survivin siRNA in treating bladder cancer, Mol Cancer Ther, 13 (2014) 71-81.

[31] M.I. Simao Carlos, K. Zheng, N. Garrett, N. Arifin, D.G. Workman, I. Kubajewska, A.A. Halwani, J. Moger, Q. Zhang, A.G. Schatzlein, I.F. Uchegbu, Limiting the level of tertiary amines on polyamines leads to biocompatible nucleic acid vectors, Int J Pharm, 526 (2017) 106-124.

[32] F. Bordi, L. Chronopoulou, C. Palocci, F. Bomboi, A. Di Martino, N. Cifani, B. Pompili, F. Ascenzioni, S. Sennato, Chitosan–DNA complexes: Effect of molecular parameters on the efficiency of delivery, Colloids and Surfaces A: Physicochemical and Engineering Aspects, 460 (2014) 184-190.

[33] L.W. Hsu, Y.C. Ho, E.Y. Chuang, C.T. Chen, J.H. Juang, F.Y. Su, S.M. Hwang, H.W. Sung, Effects of pH on molecular mechanisms of chitosan-integrin interactions and resulting tight-junction disruptions, Biomaterials, 34 (2013) 784-793.

[34] T. Sato, T. Ishii, Y. Okahata, In vitro gene delivery mediated by chitosan. effect of pH, serum, and molecular mass of chitosan on the transfection efficiency, Biomaterials, 22 (2001) 2075-2080.

[35] W.A. Larchian, Y. Horiguchi, S.K. Nair, W.R. Fair, W.D. Heston, E. Gilboa, Effectiveness of combined interleukin 2 and B7.1 vaccination strategy is dependent on the sequence and order: a liposome-mediated gene therapy treatment for bladder cancer, Clin Cancer Res, 6 (2000) 2913-2920.

[36] X. Li, S. He, Y. Tian, R.M. Weiss, D.T. Martin, Synergistic inhibition of GP130 and ERK signaling blocks chemoresistant bladder cancer cell growth, Cell Signal, 63 (2019) 109381.

[37] Y.Y. Sin, T.P. Martin, L. Wills, S. Currie, G.S. Baillie, Small heat shock protein 20 (Hsp20) facilitates nuclear import of protein kinase D 1 (PKD1) during cardiac hypertrophy, Cell Commun Signal, 13 (2015) 16.

[38] R.D. Cardiff, C.H. Miller, R.J. Munn, Manual hematoxylin and eosin staining of mouse tissue sections, Cold Spring Harb Protoc, 2014 (2014) 655-658.

[39] D.T. Martin, R.L. Gendron, J.A. Jarzembowski, A. Perry, M.H. Collins, C. Pushpanathan, E. Miskiewicz, V.P. Castle, H. Paradis, Tubedown expression correlates with the differentiation status and aggressiveness of neuroblastic tumors, Clin Cancer Res, 13 (2007) 1480-1487.

[40] M.R. Terry, R. Arya, A. Mukhopadhyay, K.C. Berrett, P.M. Clair, B. Witt, M.E. Salama, A. Bhutkar, T.G. Oliver, Caspase-2 impacts lung tumorigenesis and chemotherapy response in vivo, Cell Death Differ, 22 (2015) 719-730.

[41] W. Wang, A.M. McConaghy, L. Tetley, I.F. Uchegbu, Controls on polymer molecular weight may be used to control the size of palmitoyl glycol chitosan polymeric vesicles, Langmuir, 17 (2001) 631-636.

[42] S.A. Lewis, J.M. Diamond, Na+ transport by rabbit urinary bladder, a tight epithelium, J Membr Biol, 28 (1976) 1-40.

[43] S. Yamano, J. Dai, C. Yuvienco, S. Khapli, A.M. Moursi, J.K. Montclare, Modified Tat peptide with cationic lipids enhances gene transfection efficiency via temperature-dependent and caveolae-mediated endocytosis, J Control Release, 152 (2011) 278-285.

[44] O. Nativ, E. Dalal, G. Hidas, M. Aronson, EDTA-induced urothelial cell shedding for the treatment of superficial bladder cancer in the mouse, Int J Urol, 13 (2006) 1344-1346.

[45] K. Jezernik, O. Medalia, M. Aronson, A comparative study of the desquamation of urothelial cells during gestation and in adults mice following moderate stress or endotoxin treatment, Cell Biol Int, 19 (1995) 887-893.

[46] H. Zargar, J. Aning, J. Ischia, A. So, P. Black, Optimizing intravesical mitomycin C therapy in non-muscle-invasive bladder cancer, Nat Rev Urol, 11 (2014) 220-230.

[47] D.A. Barocas, D.R. Globe, D.C. Colayco, A. Onyenwenyi, A.S. Bruno, T.J. Bramley, R.J. Spear, Surveillance and treatment of non-muscle-invasive bladder cancer in the USA, Adv Urol, 2012 (2012) 421709.

[48] Z. Peng, Current status of gendicine in China: recombinant human Ad-p53 agent for treatment of cancers, Hum Gene Ther, 16 (2005) 1016-1027.

[49] FDA approves hereditary blindness gene therapy, Nat Biotechnol, 36 (2018) 6.

[50] H. Ledford, Gene-silencing technology gets first drug approval after 20-year wait, Nature, 560 (2018) 291-292.

[51] C. Hidai, H. Kitano, Nonviral Gene Therapy for Cancer: A Review, Diseases, 6 (2018) 1-12.

[52] J.J. Darrow, Luxturna: FDA documents reveal the value of a costly gene therapy, Drug Discov Today, 24 (2019) 949-954.

[53] V. Dodane, M. Amin Khan, J.R. Merwin, Effect of chitosan on epithelial permeability and structure, Int J Pharm, 182 (1999) 21-32.

[54] O.M. Kolawole, W.M. Lau, V.V. Khutoryanskiy, Chitosan/beta-glycerophosphate in situ gelling mucoadhesive systems for intravesical delivery of mitomycin-C, Int J Pharm X, 1 (2019) 100007.

[55] M. Huang, C.W. Fong, E. Khor, L.Y. Lim, Transfection efficiency of chitosan vectors: effect of polymer molecular weight and degree of deacetylation, J Control Release, 106 (2005) 391-406.

[56] T. Ishii, Y. Okahata, T. Sato, Mechanism of cell transfection with plasmid/chitosan complexes, Biochim Biophys Acta, 1514 (2001) 51-64.

[57] I.F. Uchegbu, L. Sadiq, A. Pardakhty, M. El-Hammadi, A.I. Gray, L. Tetley, W. Wang, B.H. Zinselmeyer, A.G. Schatzlein, Gene transfer with three amphiphilic glycol chitosans--the degree of polymerisation is the main controller of transfection efficiency, J Drug Target, 12 (2004) 527-539.

[58] E. Faizuloev, A. Marova, A. Nikonova, I. Volkova, M. Gorshkova, V. Izumrudov, Water-soluble N-[(2-hydroxy-3-trimethylammonium)propyl]chitosan chloride as a nucleic acids vector for cell transfection, Carbohydr Polym, 89 (2012) 1088-1094.

[59] C. Lonez, M.F. Lensink, E. Kleiren, J.M. Vanderwinden, J.M. Ruysschaert, M. Vandenbranden, Fusogenic activity of cationic lipids and lipid shape distribution, Cell Mol Life Sci, 67 (2010) 483-494.

[60] Z. Du, M.M. Munye, A.D. Tagalakis, M.D. Manunta, S.L. Hart, The role of the helper lipid on the DNA transfection efficiency of lipopolyplex formulations, Sci Rep, 4 (2014) 7107.

[61] C. Yu, O. Stefanson, Y. Liu, Z.A. Wang, Novel Method of Plasmid DNA Delivery to Mouse Bladder Urothelium by Electroporation, J Vis Exp, 135 (2018) 1-4.

[62] S. Horie, Y. Watanabe, R. Chen, S. Mori, Y. Matsumura, T. Kodama, Development of localized gene delivery using a dual-intensity ultrasound system in the bladder, Ultrasound Med Biol, 36 (2010) 1867-1875.

[63] R. Simon, E. Eltze, K.L. Schafer, H. Burger, A. Semjonow, L. Hertle, B. Dockhorn-Dworniczak, H.J. Terpe, W. Bocker, Cytogenetic analysis of multifocal bladder cancer supports a monoclonal origin and intraepithelial spread of tumor cells, Cancer Res, 61 (2001) 355-362.
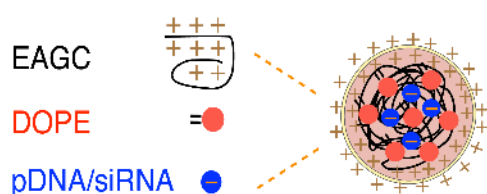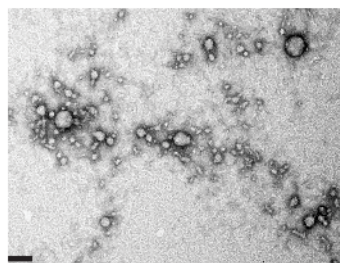
Figures

A

Properties of two distinct EAGC polymers

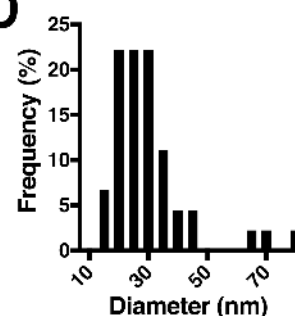| Polymers	Mole% substitution (moles of ethylamino per 100 moles of monomer)	Molecular weight (Mw, kDa)	Polydispersity index (Mw/Mn, PDI)
EA25GC45	25.0	45.0	1.027
EA28GC83	28.0	83.0	1.016

B

EAGC
DOPE
pDNA/siRNA

C

D

Figure 1. Characterization of the EAGC polymers. (A) The % mole ethylamino substitution, molecular weight, and the polydispersity of the polymers. **(B)** Schematic representation of EAGC-DOPE lipid hybrid nanoparticles (EGCDNPs). **(C)** Transmission electron microscopy (TEM) image demonstrated the structure of the hybrid NPs proposed in **(B)**. **(D)** Size distribution of EGCDNPs measured from the TEM image in **(C).** Scale bar = 100 nm.
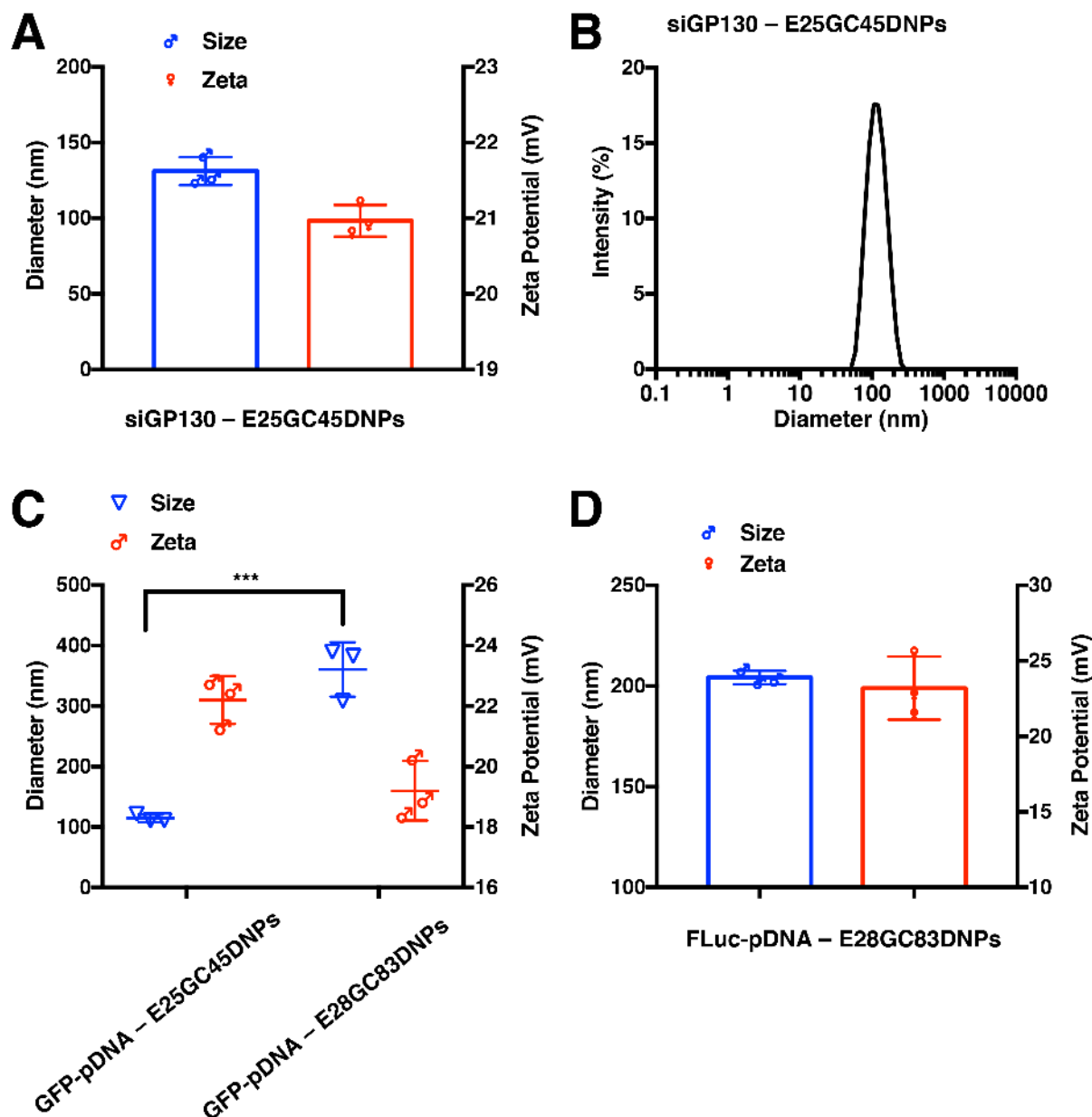
Figure 2. Characterization of pDNA/siRNA – EGCDNPs. (**A**) Size and zeta potential of siGP130 formulated with E25GC45DNPs at an EGCDNPs, siRNA mass ratio of 20:1. (**B**) A representative image for the size measurement of siGP130 – E25GC45DNPs. (**C**) Size and zeta potential of E25GC45DNPs and E28GC83DNPs when complexed with GFP-pDNA at an EGCDNPs, pDNA mass ratio of 10:1 measured by DLS. *** represents $p < 0.001$, the significant difference between the size of E25GC45DNPs – GFP-pDNA and E28GC83DNPs – GFP-pDNA. (**D**) Size and zeta potential of E28GC83DNPs – FLuc-pDNA complexes (EGCDNPs, pDNA mass ratio of 10:1).
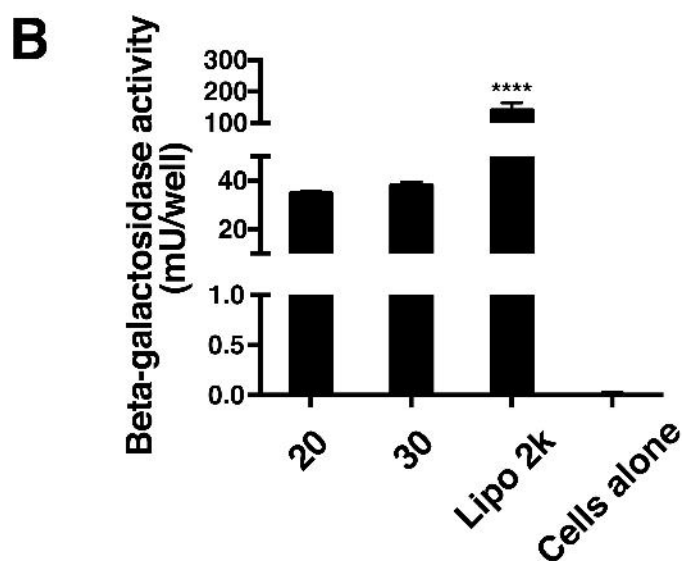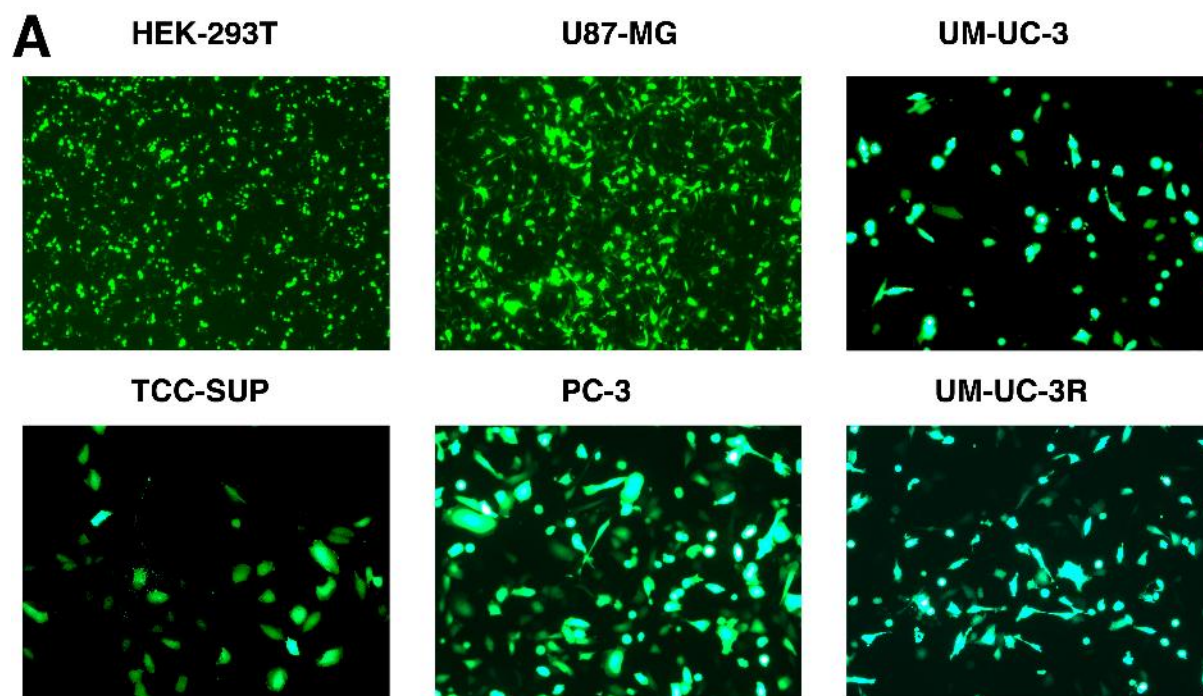
Figure 3. EGCDNPs-enabled pDNA transfection in multiple cell types. (A) Representative fluorescence images of cells after transfection for 4 h with EGCDNPs, GFP-pDNA mass ratio of 10:1 (HEK-293T), 10:1 (UM-UC-3), 10:1 (UM-UC-3R) and 10:1 (TCC-SUP) or 6 h with EGCDNPs, GFP-pDNA mass ratio of 40:1 (U87-MG), 20:1 (PC-3), followed by a 48 h recovery phase for UM-UC-3, UM-UC-3R, and PC-3 or a 72 h recovery phase for HEK-293T, U87-MG, and TCC-SUP. All images are shown at x100 magnification except for the fact that the images for HEK-293T and U87-MG cells are taken under the x40 magnification. **(B)** β-

galactosidase activity of HEK-293T cells after administration of E25GC45DNPs – β-gal-pDNA complexes at EGCDNPs, pDNA mass ratios of 20 or 30:1 when compared to Lipo 2k (**** $p < 0.0001$) and cells alone. All treatments were dosed with 4 µg of β-gal-pDNA. Data are presented as mean ± SD ($n = 3$).
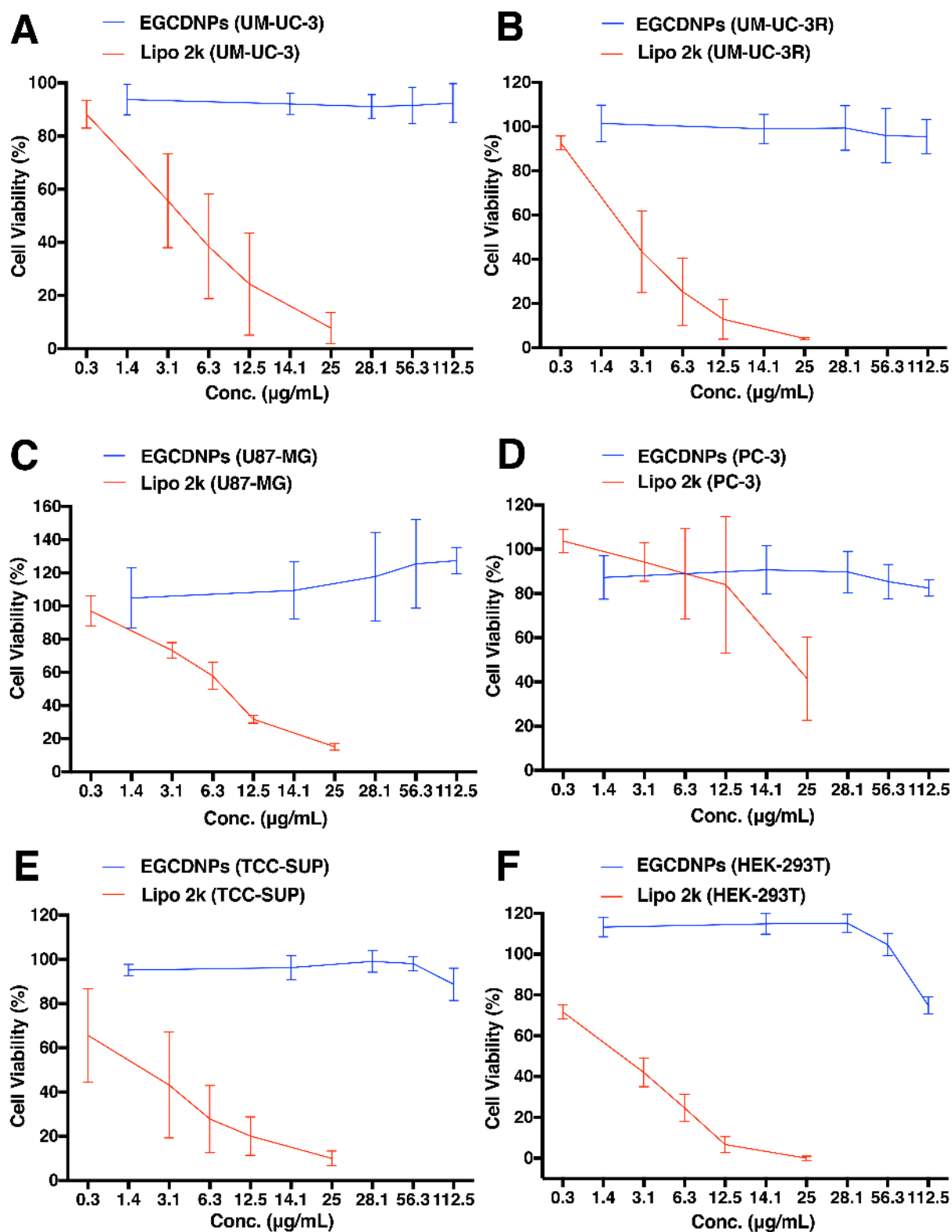
Figure 4. A comparison of the cytotoxicity of Lipo 2k and E25GC45DNPs in multiple cell lines. A cell viability (WST-1) assay was used with different concentrations of E25GC45DNPs or Lipo 2k for 6 h followed by a 48 h recovery phase for all cell lines except for 72 h for PC-3

and TCC-SUP cells. Data are presented as the mean ± SD of three independent experiments with five replicates each. The concentration of EGCDNPs is calculated as the combined concentration of polymer and lipid.
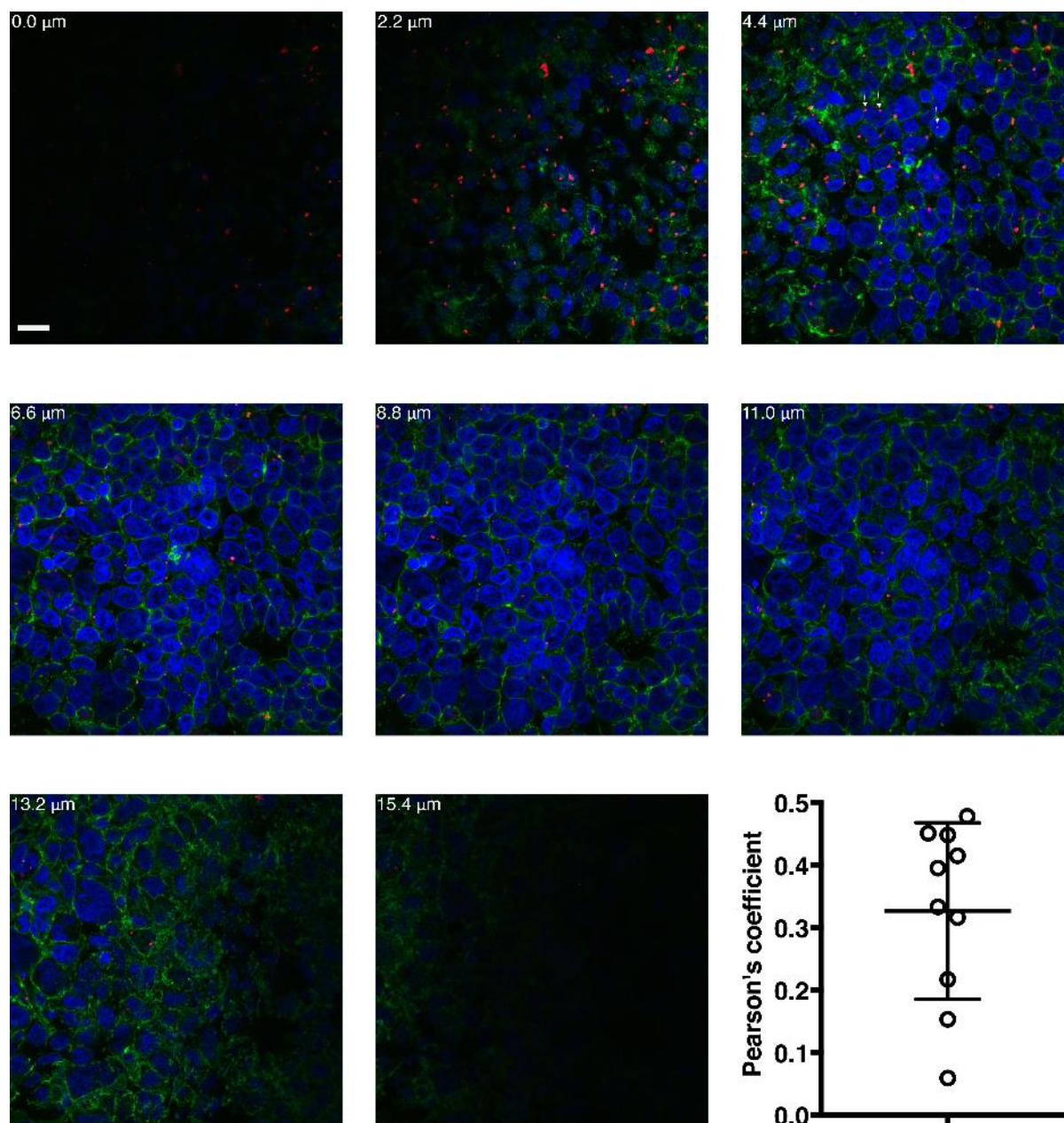
Figure 5. EGCDNPs not only shuttle pDNA into the perinuclear region but also induce pDNA nuclear transfer after 4 h of treatment. HEK-293T cells were treated with E25GC45DNPs formulated with Cy5-labelled GFP-pDNA at an EGCDNPs, pDNA mass ratio of 40:1 for 4 h (1 μg/well of Cy5-labelled GFP-pDNA). Cy5-labelled GFP-pDNA was observed to accumulate in the perinuclear and nuclear regions (white arrows). GFP-pDNA was labelled with the Cy5 (red), the nuclei were stained with Hoechst (blue), and actin was stained with CF®488A-phalloidin (green). A confocal z-stack was performed, and images were taken

of eight consecutive slides (2.2 μm distance per slide). Pearson's coefficient denotes the fraction of Cy5-labelled GFP-pDNA (red) overlapping with the nuclei labelled with Hoechst (blue). Data are presented as mean ± SD ($n = 10$). Scale bar = 20 μm.
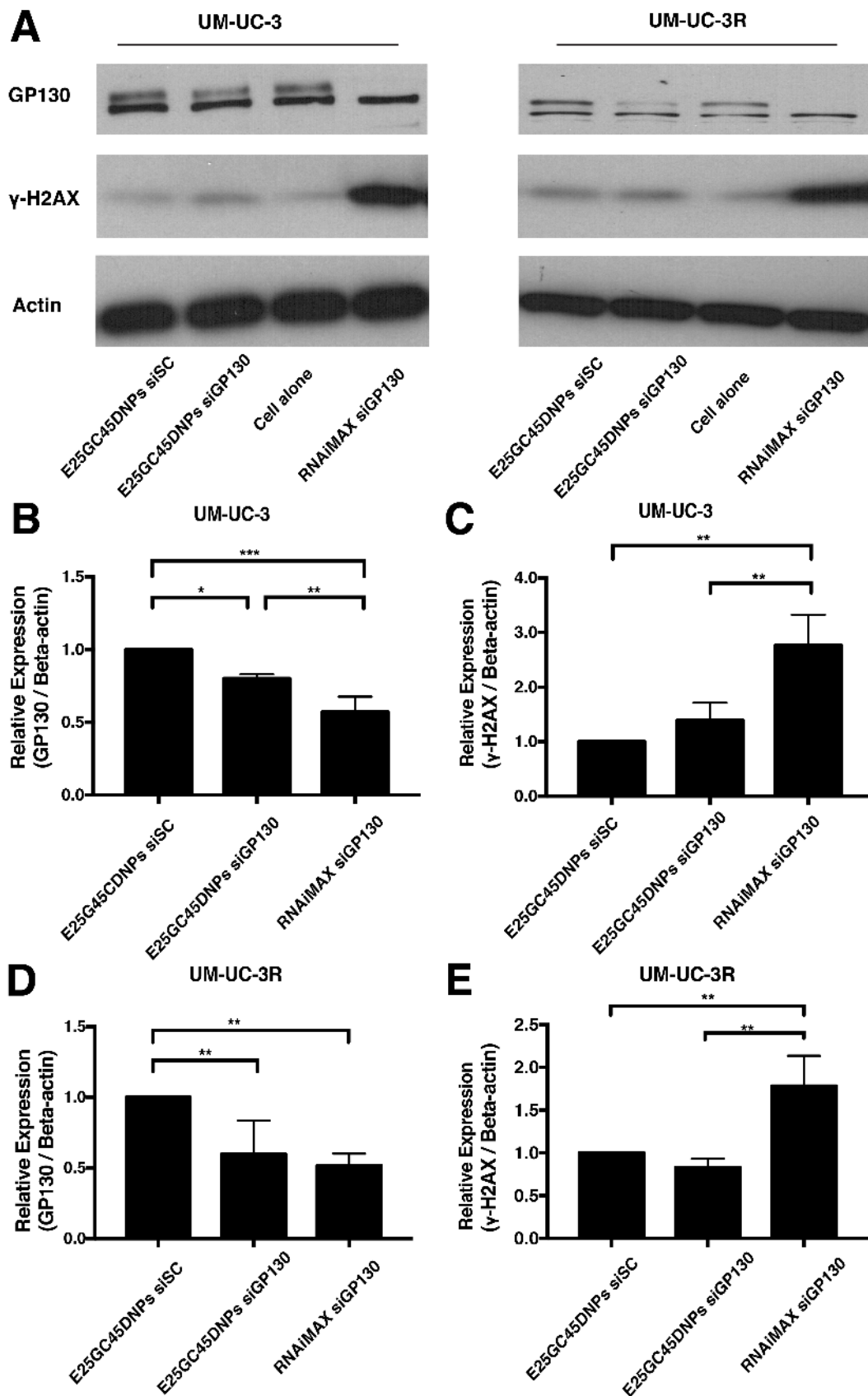
Figure 6. GP130 protein downregulation mediated by EGCDNPs and Lipofectamine RNAiMAX loaded with siGP130 in UM-UC-3 and UM-UC-3R cells. (A) GP130 and γ-

Figure 6. GP130 protein downregulation mediated by EGCDNPs and Lipofectamine RNAiMAX loaded with siGP130 in UM-UC-3 and UM-UC-3R cells. (A) GP130 and γ-

41

H2AX protein levels assessed by western blot for UM-UC-3 and UM-UC-3R human bladder cancer cells treated with siGP130 – E25GC45DNPs, siGP130 – Lipofectamine RNAiMAX, or scrambled siRNA (siSC) – E25GC45DNPs at a dose of 4 μg/well siRNA. **(B–E)** The relative GP130/γ-H2AX expression levels of UM-UC-3 and UM-UC-3R cells are shown. Protein levels were normalized using beta-actin and the data are shown as mean ± SD of three to four independent experiments. * represents $p < 0.05$, ** represents $p < 0.01$, and *** represents $p < 0.001$.
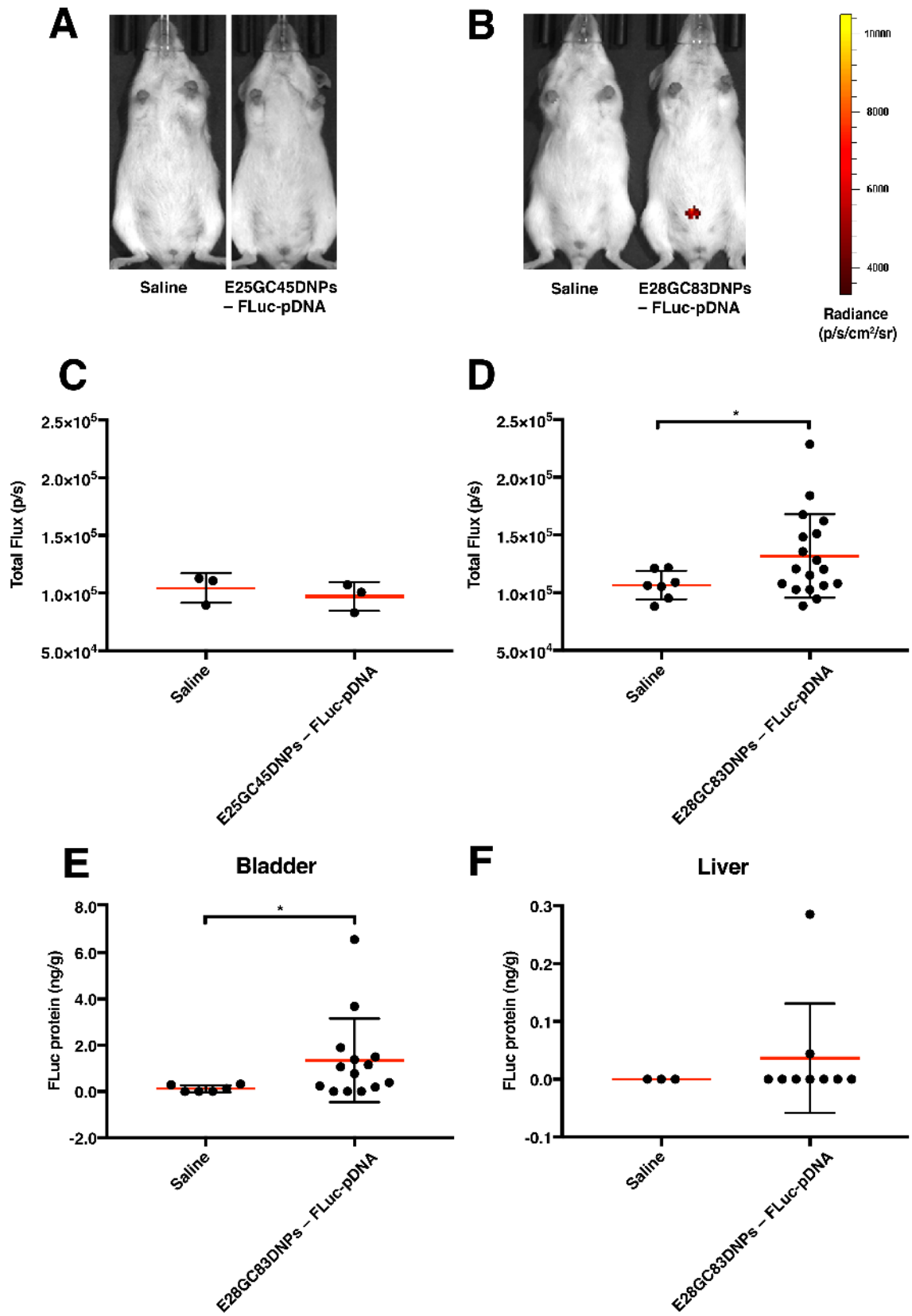
Figure 7. Intravesical instillation of E25GC45DNPs and E28GC83DNPs encapsulating firefly luciferase plasmid DNA (FLuc-pDNA) in the murine bladder. Representative

images of bioluminescence after instillation of two doses of **(A)** E25GC45DNPs and **(B)** E28GC83DNPs encapsulating pDNA (encoding Firefly luciferase; 6.4 µg FLuc each) over 48 h. Quantification of luminescence by IVIS **(C)** FLuc-pDNA – E25GC45DNPs ($n = 3$; vs saline groups, $n = 3$) and **(D)** FLuc-pDNA – E28GC83DNPs ($n = 18$; vs saline groups, $n = 7$). Luminescence extracted from **(E)** bladder and **(F)** liver tissues following the treatment with FLuc-pDNA – E28GC83DNPs [$n = 14$ in **(E)** or $n = 9$ in **(F)**] in comparison with the saline group [$n = 6$ in **(E)** or $n = 3$ in **(F)**]. * $p < 0.05$. Data are shown as mean ± SD.
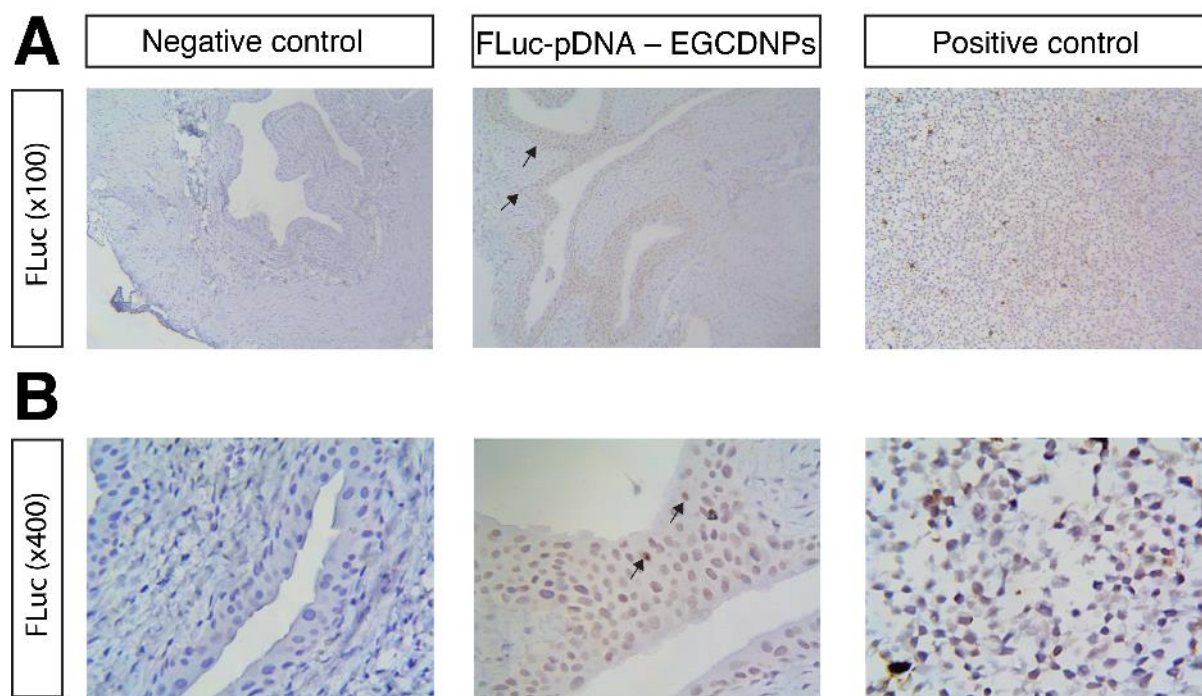
Figure 8. Immunohistochemistry of firefly luciferase expression in the murine bladder. Murine bladders were treated with FLuc-pDNA – E28GC83DNPs complexes. Paraffin-embedded human UM-UC-3 cell pellets treated with E25GC45DNPs encapsulating FLuc-pDNA were used as a positive control for luciferase staining whereas negative controls for luciferase staining included murine bladder sections with only secondary antibody staining. FLuc-pDNA – E28GC83DNPs-treated groups induced firefly luciferase expression in the urothelium and lamina propria regions (black arrows). Images were acquired at x100 **(A)** and x400 **(B)** magnification.
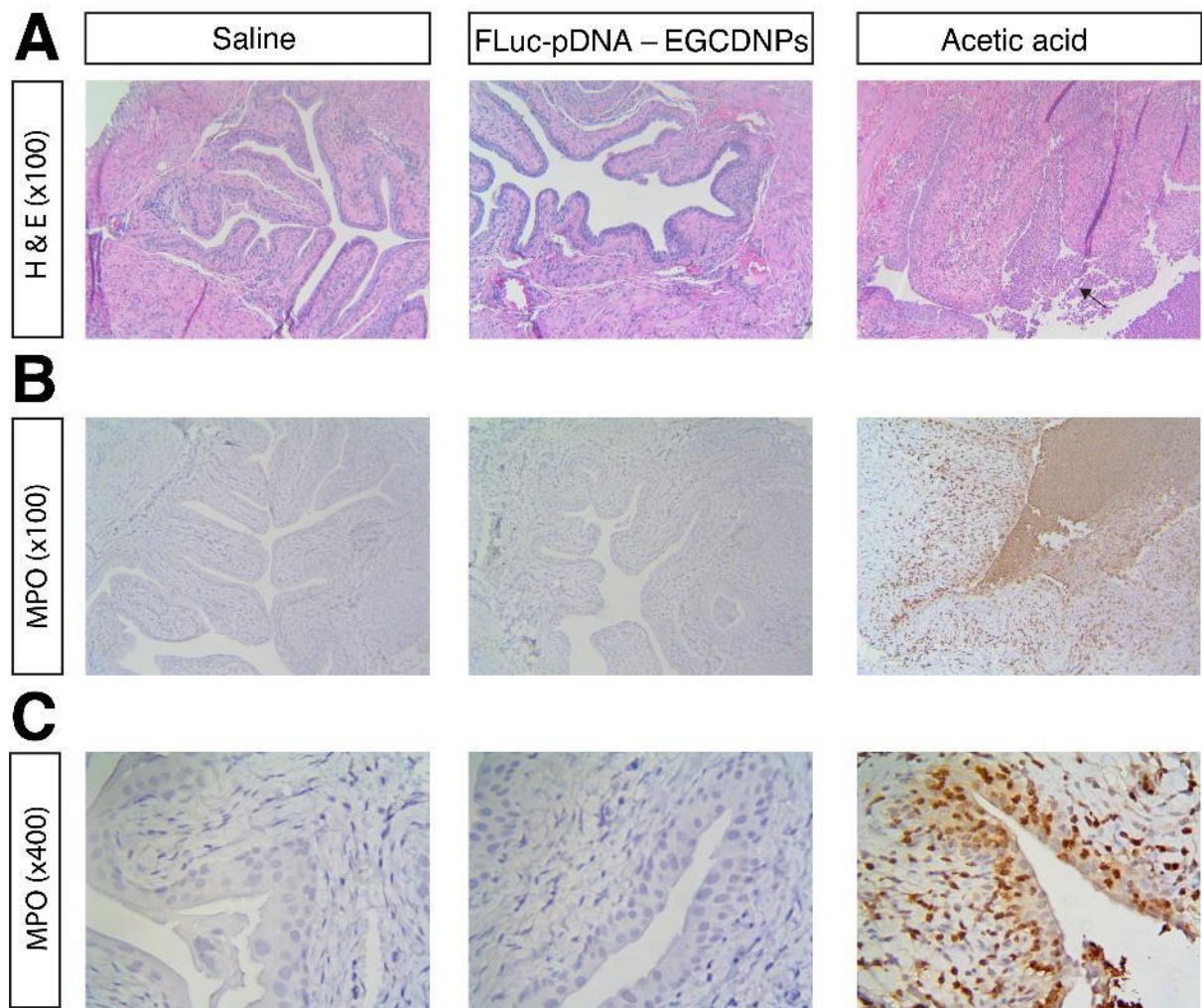
Figure 9. EGCDNPs complexing with firefly luciferase plasmid DNA (FLuc-pDNA) showed no adverse effects on the bladder, *in vivo*. (A) Histopathological analysis of bladder tissue sections after treatment with saline, E28GC83DNPs complexes (6.4 µg FLuc-pDNA per dose, twice in total), and positive control (acetic acid-treated rat bladders). Immunohistochemistry was performed for myeloperoxidase (MPO). The black arrow indicates the damaged urothelial cells. All images are shown at x100 **(A–B)** or x400 **(C)** magnification.
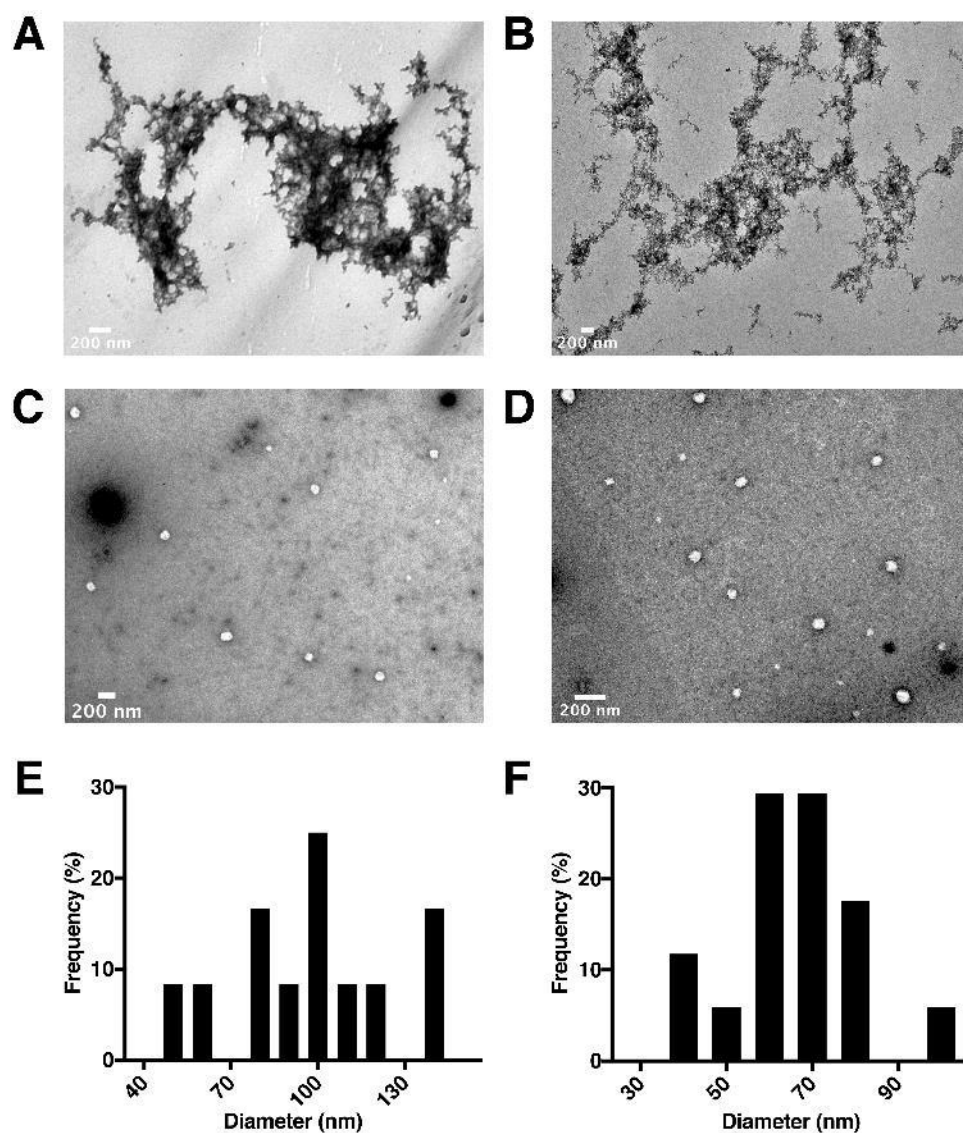
Supplementary Fig. S1

Transmission electron microscopy (TEM) for morphology and size of EGCDNPs. (A) Naked siGP130, (B) naked GFP-pDNA, (C) E25GC45DNPs formulated with siGP130 at an EGCDNPs, siRNA mass ratio of 20:1, and (D) E25GC45DNPs complexing with GFP-pDNA at an EGCDNPs, pDNA mass ratio of 10:1. (E) Size distribution of GP130 siRNA –

E25GC45DNPs complexes measured from the TEM image in (C). (F) Size distribution of GFP pDNA – E25GC45DNPs complexes measured from the TEM image in (D). Scale bar = 200 nm.
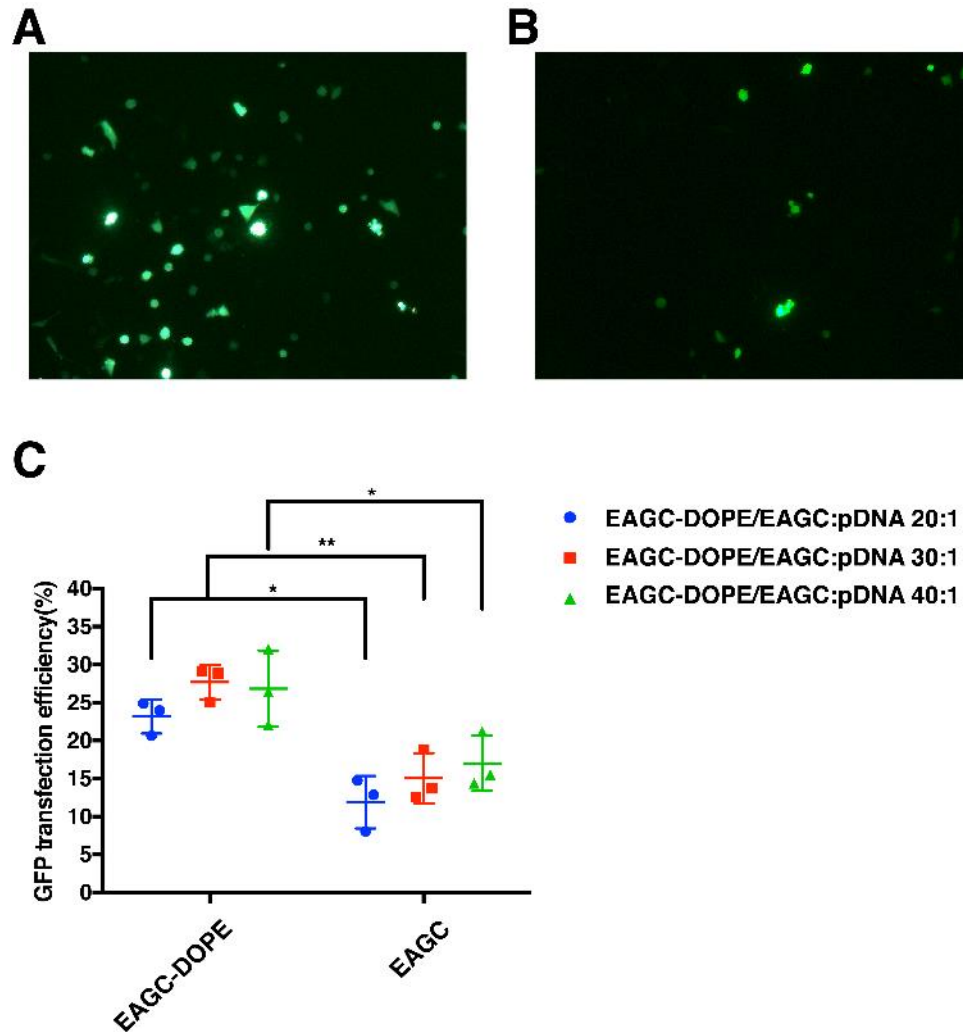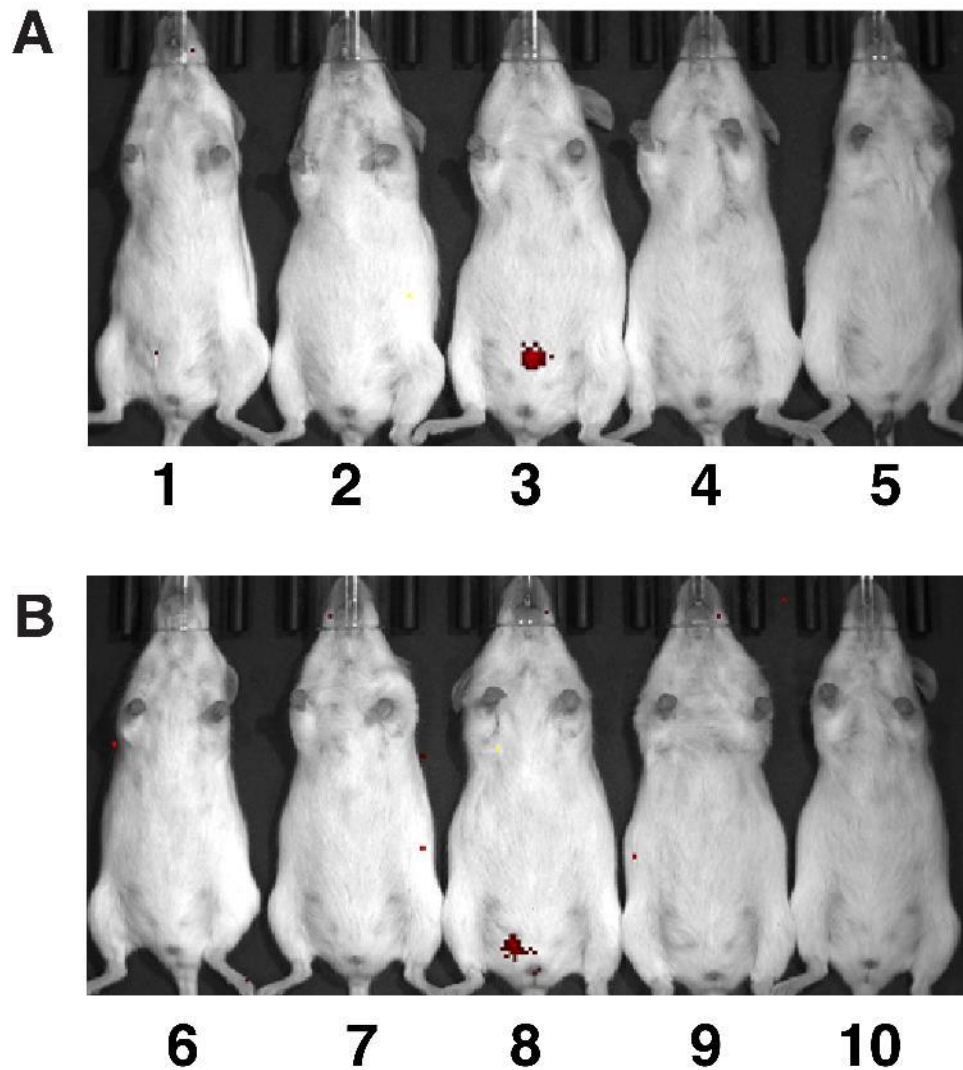

Supplementary Fig. S2

A comparison between EGCDNPs and EAGC in transfecting GFP-pDNA in UM-UC-3 and U87-MG cells. The fluorescence images of UM-UC-3 cells after transfection of EGCDNPs complexes (A) or EAGC complexes (B) as vectors; GFP-pDNA (1.6 µg/well) mass ratio of 40:1 (at x100 magnification). GFP transfection efficiency also was quantified in U87-MG cells following treatment comprised of EGCDNPs/EAGC and GFP-pDNA (1.6 µg/well) with mass ratios of 20:1 (blue, circle), 30:1 (red, square) and 40:1 (green, triangle) (C). The results are

expressed as the percentage of GFP positive cells versus total cell population of U87-MG cells where * represents $p < 0.05$, and ** represents $p < 0.01$. Data are shown as mean ± SD ($n = 3$).
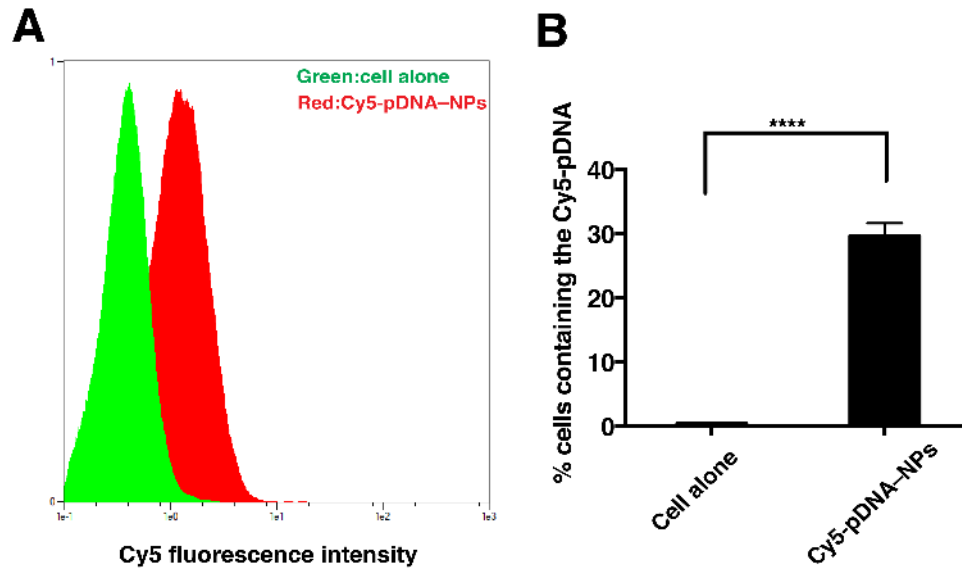
Supplementary Fig. S3

Cellular uptake of GFP-pDNA. (A) Histogram of the Cy5 channel from non-treated (green) and Cy5-labelled GFP-pDNA complexed with E25GC45DNPs (at an EGCDNPs, GFP-pDNA mass ratio of 40:1, 1 μg GFP-pDNA/well) channel (red) after 4 h of treatment in HEK-293T cells. (B) The percentage of Cy5 positive cells was quantified by flow cytometry. Data are shown as mean ± SD ($n = 3$). **** represents $p < 0.0001$.

Supplementary Fig. S4

The effect of incorporating chloroquine in augmenting EGCDNPs' gene transfection *in vivo* healthy murine bladder. (A) Bioluminescence images of mice 24 h post treatment. Mice were intravesically instilled with complexes containing FLuc-pDNA (2.4 μg) and EGCDNPs (26.4 μg) or with lipoplexes containing Lipo 2k (6 μg) and FLuc-pDNA (2.4 μg). Additionally, 3.4 μg of chloroquine (CQ) was added to the EGCDNPs complexes as described previously. Lane descriptors: 1 – Lipoplexes (Lipo 2k), 2 – E25GC45DNPs complexes plus CQ, 3 – E28GC83DNPs complexes plus CQ, 4 – E25GC45DNPs complexes without CQ, 5 – E28GC83DNPs complexes without CQ. (B) Bioluminescence images of mice 48 h post treatment with each mouse dosed once per day over 48 h with 2.4 μg of FLuc-pDNA complexed

with EGCDNPs (26.4 μg) by intravesical instillation. Additionally, 3.4 μg of chloroquine was added to the EGCDNPs complexes. Lane descriptors: 6 – saline control, 7 – E28GC83DNPs complexes without CQ, 8 – E28GC83DNPs without CQ, 9 – E28GC83DNPs complexes with CQ, 10 – E28GC83DNPs complexes with CQ.

Cell lines	Lipo 2k (IC$_{50}$, μg/mL)	EGCDNPs (% cell viability at the IC$_{50}$ of Lipo 2k)
UM-UC-3	3.71 ± 1.40	More than 92%
UM-UC-3R	2.51 ± 0.76	More than 99%
U87-MG	7.27 ± 0.78	More than 99%
PC-3	22.22 ± 5.78	More than 90%
TCC-SUP	1.20 ± 0.86	More than 95%
HEK-293T	1.32 ± 0.43	More than 99%

Supplementary Table S1

IC$_{50}$ for Lipo 2k and % cell viability with respect to EGCDNPs at the IC$_{50}$ for Lipo 2k in six tested cell lines.